Chapter 1

Introduction

Preface

This research has been undertaken as part of a collaborative project with BlueScope Steel®, an Australian-based steel company, and Quaker Chemical (Australasia), a company which manufactures specialty lubricants, including many of the cold rolling oils used by BlueScope Steel®. The primary focus has been to gain an improved understanding of relationships between cold rolling oil composition and residue-forming characteristics and the occurrence of uncoated defects in 55Al-43.4Zn-1.6Si hot dip metallic coatings. The Chapter is divided into three sections, the first of which provides a description of the industrial context within which this research has been conducted. Overviews of the steel cold rolling and continuous hot dip metallic coating processes employed BlueScope Steel® at its Springhill works are provided, together with information on the general make-up and properties of cold rolling oils.

The second section reviews the literature concerning:

- 55Al-43.4Zn-1.6Si hot dip metallic coatings and uncoated defects;
- the process of, and key techniques for, studying residue formation in cold rolling oils and other lubricating oils and greases, and
- the thermal decomposition and residue-formation reactions undergone by three key classes of rolling oil ingredients, base esters, sulfurised extreme-pressure (EP) additives and phosphorus-based lubrication additives.

In the final section, an overview of the aim and scope of this thesis, together with an outline for its structure, are provided.

1.1 Industrial Context

1.1.1 Significance of Australian Metal Coated Steel Products

Australia's steel industry plays a key role in global steel production and the Australian

economy. In 2002 Australia produced 7625 kt of steel, accounting for 0.85 % of the world's total steel production for that year and turning over approximately A$21.1 billion.[1] BlueScope Steel® produced 5000 kt, or 66 % of this total, making it the world's 28th largest steel producer and Australia's largest steel production company by product mass, as shown in figure 1.1.[1]

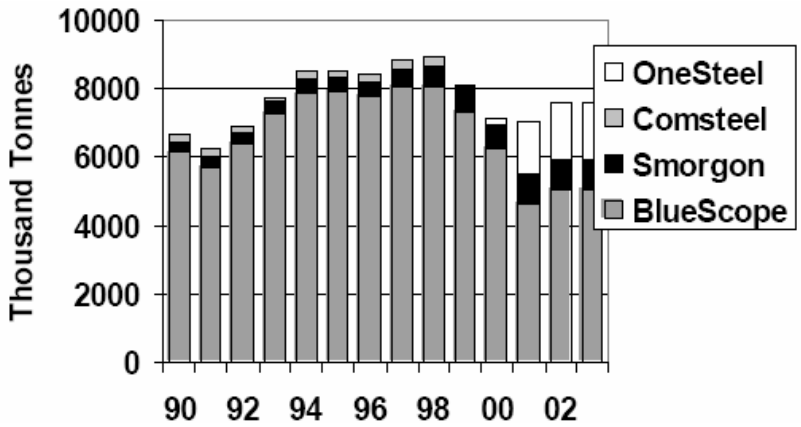

Figure 1.1 Australian steel production by company for 1990–2003.[1]

Today, BlueScope Steel®'s metal-coated cold rolled products, such as Colorbond®, Zincalume® and Galvalume®, comprise approximately 40 % of the company's total production figure[2] and have become popular Australian brand names over the past forty years. In fact, coated steel products comprise a major part of Australian exports and are BlueScope Steel®'s second most lucrative product class. In 2005/2006 approximately 2199 kt of coated steel products were externally despatched, 650 kt of which were exported. The total revenue yielded from the sale of these products was A$3.06 billion.[2] Given these statistics, it becomes evident that the production of high quality coated steel products by BlueScope Steel® is of utmost importance to both the success of the company and to Australia's economy.

1.1.2 The Steel Cold Rolling Process

The majority of BlueScope Steel®'s metal coated sheet products are produced using

G550-grade cold rolled steel. This type of steel has low ductility and high strength and is used to make building products such as roofing.[3] A summary of the typical dimensional, mechanical and chemical properties of G550 steel is given in table 1.1.

Table 1.1 Dimensional, mechanical and chemical properties of cold rolled steels within the G550 range.[3]

Thickness (mm)	Max. Strip Width (mm)	Yield Strength Range (MPa)	Tensile Strength Range (MPa)
0.35	1150-1220	690-790	730-790
0.42	1235	680-780	710-790
0.48	1235	670-750	700-760
0.55	1235	650-740	680-750
0.75	1220	600-690	650-710
1.0	1220	570-640	610-670
Typical Chemical Composition of Steel Base (%)			
Carbon		0.035-0.070	
Phosphorus		0.00-0.02	
Manganese		0.20-0.30	
Sulfur		0.00-0.02	
Silicon		0.00-0.02	
Aluminium		0.02-0.07	
Nitrogen		0.000-0.008	

Figure 1.2 shows a schematic diagram of the cold rolling process at BlueScope Steel®'s Springhill works. The process begins with hot rolled steel stock being cracked to loosen surface oxides and welded to the end of the previous sheet. The new sheet passes through the pickle entry accumulator, which stores an excess of sheet so that the Cold Rolling Mill (CRM) can be continuously fed whilst a new sheet of steel is being welded.

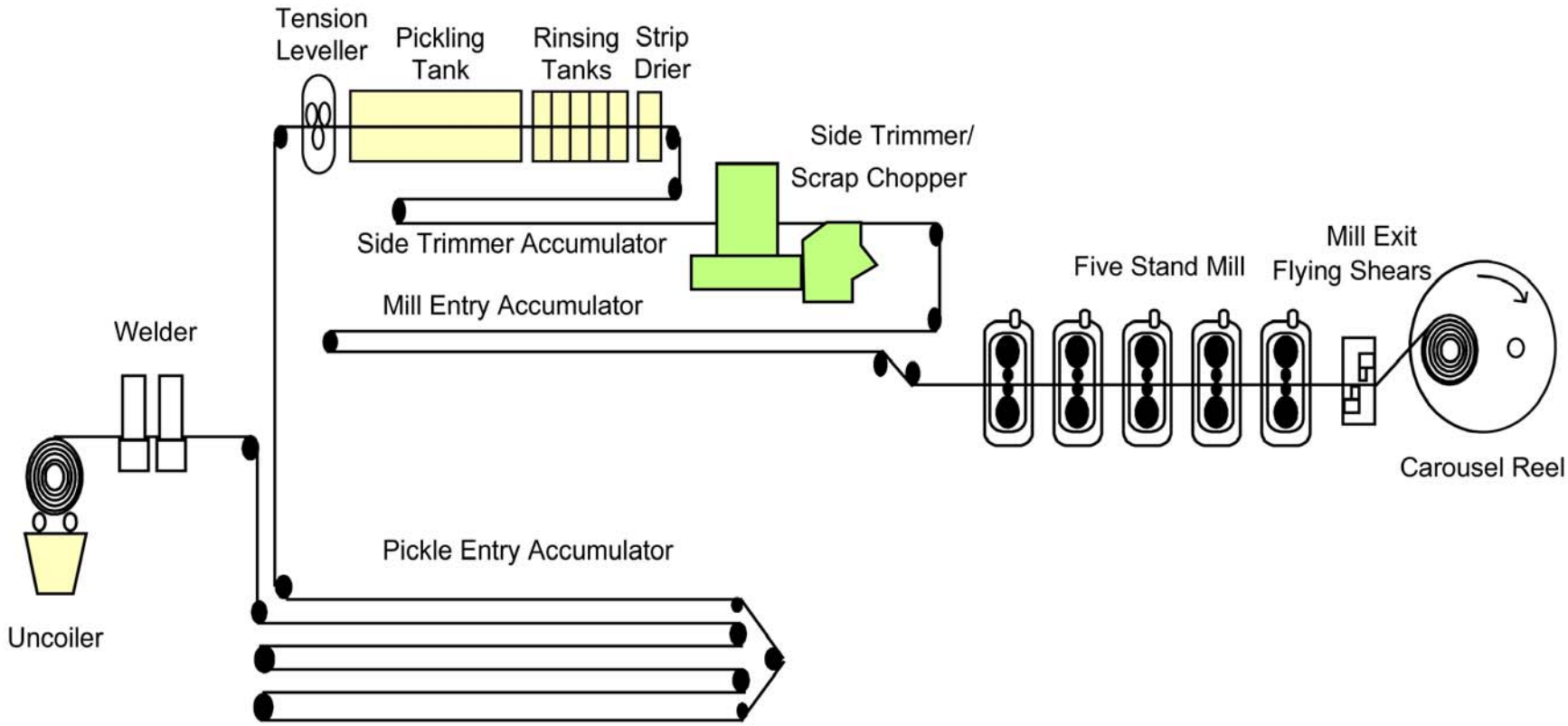

Figure 1.2 Schematic diagram of the cold rolling process employed at BlueScope Steel®'s Springhill works.

The sheet is then tension levelled before entering the pickling tank, which contains a 10 % w/v hydrochloric acid solution, to remove surface oxides (scheme 1.1).[4]

$$Fe_3O_{4(s)} + Fe_{(s)} + 8HCl_{(aq)} \leftrightarrow 4FeCl_{2(aq)} + 4H_2O_{(aq)}$$

Scheme 1.1 Reaction undergone by the steel substrate during 'pickling'; iron/iron oxide present on the steel surface reacts with hydrochloric acid solution to form iron chloride and water.

After pickling, the sheet is passed through a series of water rinsing tanks and a drier before being trimmed and passed onto the mill entry accumulator.

At the Springhill CRM, the sheet undergoes a series of five reductions in thickness by passing through five different sets of rollers. The magnitude of these reductions is dependent on the desired product dimensions. Each roller set contains two working rollers, which come into contact with the steel surface, and two backup rollers, which apply a load to the working rollers. The point at which the working rollers come into contact with the steel strip is known as the roll bite. The temperature of the steel sheet as it passes through the first roll bite is approximately 250 ^{o}C. This value is lowered to 110-120 ^{o}C by the time the sheet reaches the last stand of rollers in the mill. The sheet is fed into the rollers at approximately 170 m min^{-1} and an oil emulsion (3-4 % rolling oil in water, manufactured by Quaker Chemical Australasia) is sprayed onto the sheet surface between each roller set. The oil plates out onto the steel to form a film several hundred nanometers thick (corresponding to an oil mass of ~ 600 mg m^{-2})[5] and the water in the emulsion evaporates, cooling the steel surface. Small metallic particles are generated by wear between the working rolls and the steel surface and remain within the rolling oil film at concentrations in the range 20-50 mg m^{-2}.[5] The steel sheet is tensioned between the roller sets and is fed out at approximately 200 m min^{-1}. This higher speed results from the creation of fresh metal surface during the rolling process as a result of the reduction in strip thickness; the increased metal surface area makes the steel sheet longer as opposed to wider. Steel coming out of the CRM is coiled into 12000-30000 t coils, which can be stored for up to a week before further treatment. During this storage time

the coils are said to undergo an 'aging' process, whereby chemical reactions occur between the steel surface/iron fines, the residual rolling oil and any water/gases trapped in the coil.[6-8]

1.1.3 Cold Rolling Oils

Rolling oils used in the cold rolling of steel sheet are required to possess a range of properties that enable them perform a specific set of functions.[9] Not only must rolling oil possess appropriate emulsion-forming, lubrication and corrosion protection properties; it must also be easily removed from the strip surface prior to the application of the hot dip metallic coating.

In order to achieve good lubrication during the cold rolling process, the rolling oil must be able to accommodate high compression and tension forces as well as the creation of fresh metal surfaces. These lubrication requirements mean that the rolling oil must have an appropriate pressure-viscosity coefficient so that it remains fluid enough to spread over the new steel surface created during the reduction process whilst providing the working rolls with good lubrication under the loads used.[9] In addition, due to the high temperatures and pressures used during cold rolling and the fact that rolling oils are often recycled in emulsion re-circulation systems (the rolling oil used at the Springhill works is recycled in such a system), the oil must be resistant to thermal degradation, polymerisation and hydrolysis. Consequently, synthetic di- and tri-ester derivatives of natural vegetable oils are commonly used as the basis of rolling oil formulations.[9-11] Numerous different additives, including free fatty acids, emulsifiers and mineral oil together with minor additives such as anti-oxidants, lubrication additives, viscosity boosting agents and corrosion inhibitors are then blended into the base oil to construct a fully-formulated cold rolling oil.[12] The concentration and chemical nature of these additives are unique to the requirements of the CRM in question; no two CRM's use exactly the same rolling oil.

1.1.4 The Continuous Hot Dip Metallic Coating Process

The most common method by which 55Al-43.4Zn-1.6Si coatings are applied to the surface of cold rolled steel is the continuous hot dip coating process (figure 1.3).[13, 14] The first step in continuous hot dip coating involves seam welding the end of a new cold rolled coil to the end of the coil being processed. The new coil is then fed into the entry accumulator before being passed through a pre-heater which heats the steel sheet to ~ 200 ^{o}C.[15] Following this, the sheet enters the 'continuous annealing' cleaning section which incorporates a dual furnace system. Removal of the thin rolling oil layer deposited on the steel surface by the cold rolling process occurs within the Direct Fired Furnace (DFF), which contains several zones fired under either natural gas combustion products or nitrogen. The heating rates within the DFF are estimated to be approximately 6500 ^{o}C min^{-1} and the final steel surface temperature is approximately 500 ^{o}C.[7]

Although theoretical studies have shown that the non-equilibrium conditions present in the DFF (whilst the steel surface is at ~ 500 ^{o}C, the surrounding gas is at ≥ 1000 ^{o}C) result in the furnace atmosphere being reducing to steel,[15] the steel is subsequently passed through the Reduction Furnace (RF), which contains a low dew point, hydrogen-nitrogen (HNX) atmosphere under which surface oxides are reduced (scheme 1.2.).[15]

$$Fe_3O_{4(s)} + 4H_{2(g)} \leftrightarrow 3Fe_{(s)} + 4H_2O_{(g)}$$

Scheme 1.2 Reaction of steel surface oxides with hydrogen gas within the RF; iron oxide is reduced to metallic iron, giving off water as a by-product.

The continuous annealing process offers several advantages over other cleaning methods such as alkaline, acid and electrolytic degreasing. Furnace treatment enables simultaneous cleaning of the steel surface, modification of the physical properties of the steel and pre-heating prior to entry into the metal coating bath. Incorporation of the furnace cleaning section into the hot dipping line enables the process to be continuous, maximising throughput. Furthermore, the continuous annealing process is less time consuming than the alternative furnace cleaning process of 'batch annealing'.

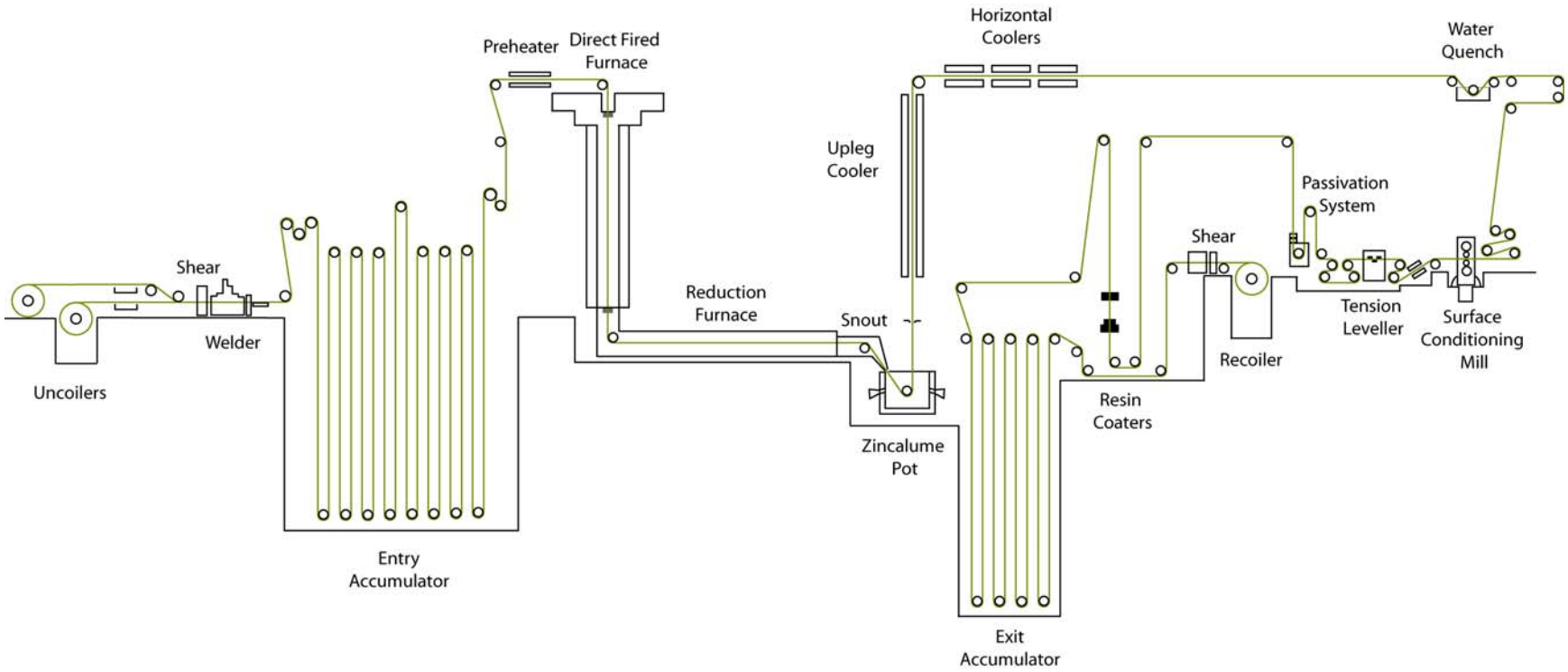

Figure 1.3 Schematic diagram of the continuous hot dip metallic coating process employed at BlueScope Steel®'s Springhill works.

Batch annealing involves stacking cold rolled coils within a furnace containing hydrogen or HNX gas and heating at slow (1.7 ^{o}C min^{-1}) heating rates to approximately 690 ^{o}C.[16, 17] The coils are subsequently cooled before being coated in a separate process. Following the continuous annealing section, the steel sheet is pulled through the 'Zincalume® pot', a coating bath containing the molten 55Al-43.4Zn-1.6Si alloy (figure 1.4). Air knives at the bath exit control the coating thickness and the rate of solidification. The metal-coated sheet then undergoes several post-bath treatments, including surface conditioning, tension levelling, passivation and resin coating, before it is re-coiled and cut.

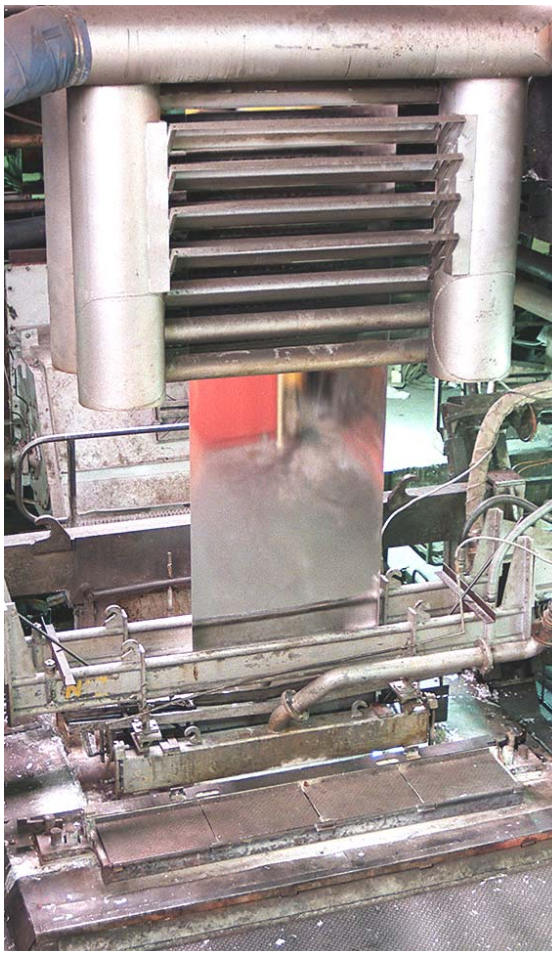

Figure 1.4 Photograph of alloy-coated steel strip exiting the metal coating bath at BlueScope Steel®'s Springhill works.

1.2 Literature Review

1.2.1 55Al-43Zn Hot Dip Metallic Coatings

1.2.1.1 Coating Structure and Properties

Zinc-based metallic coatings have been used since the early 1800's to protect steel products from corrosion.[18] The corrosion protection afforded by these coatings is two-fold. Zinc has a lower standard potential than iron[19] and will preferentially undergo oxidation so that zinc-based coatings provide galvanic protection to steel. Furthermore, the products created by the sacrificial oxidation of zinc-based coatings tend to form a dense, inert layer that constitutes a physical barrier to steel substrate oxidation.[14, 20]

There are many different types of zinc-based coatings used within the steel industry. Some of the typical coating classes include zinc (galvanised), zinc-iron (galvanneal), zinc-5 % w/w aluminium (Zn-5Al) and zinc–55 % w/w aluminium (Zn-55Al).[20] Traditionally, galvanised coatings have been the most widely used of all these coating classes,[20] however the Zn-55Al type coatings, including Zincalume®, or 55Al-43.4Zn-1.6Si, have recently become increasingly popular within the building and manufacturing industries.[14] Not only do 55Al-43.4Zn-1.6Si coatings have excellent aesthetic qualities as a result of their fine, uniform spangles (figure 1.5) but they combine the durability of aluminium coatings with the corrosion resistance properties of zinc.[14, 20]

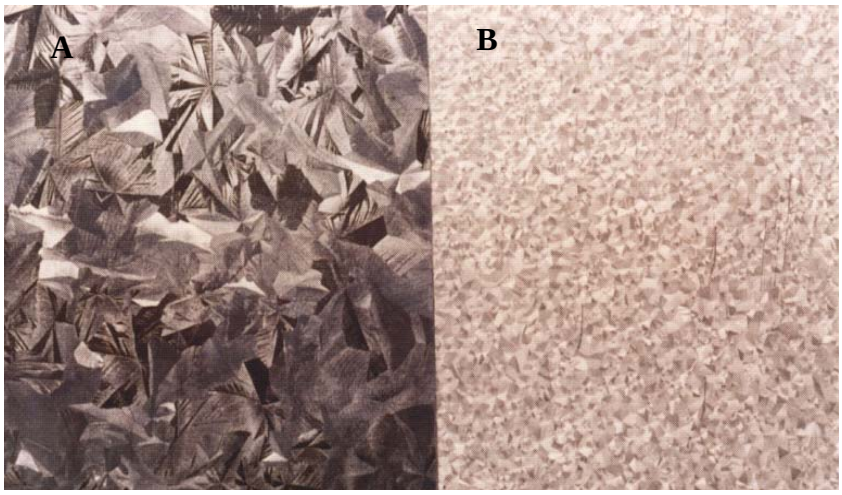

Figure 1.5 Photographs of typical galvanised (A) and Zincalume® (B) coatings.

Zincalume®-coated steel is characterised by three bulk layers; the steel substrate, a thin (1-2 μm thick) iron-aluminium-zinc intermetallic layer and a 20-25 μm thick 55Al-43.4Zn-1.6Si alloy layer (figure 1.6).[20]

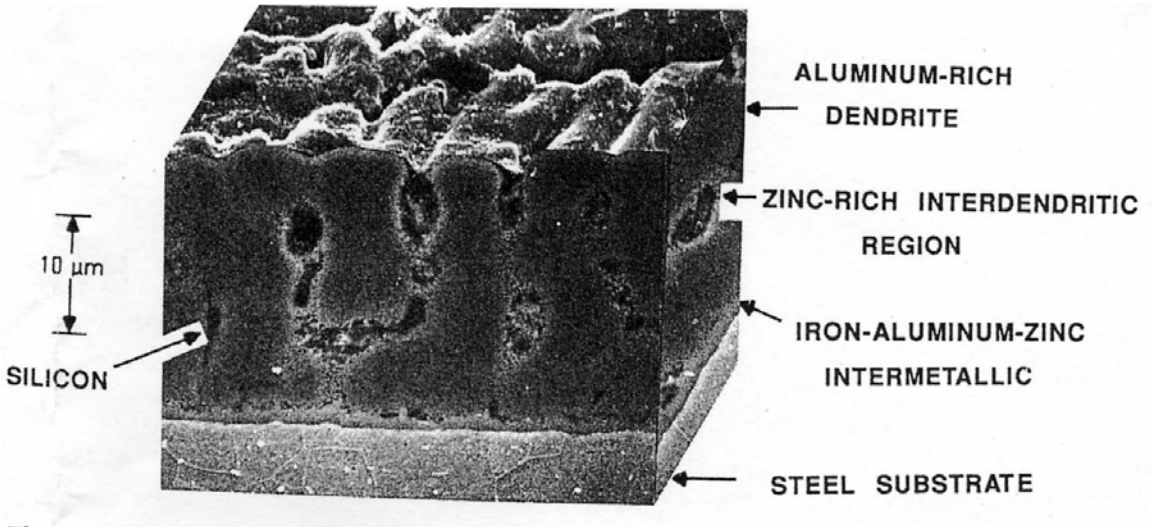

Figure 1.6 SEM image showing 55Al-43.4Zn-1.6Si coating microstructure.[20]

The intermetallic layer is formed by the liquid/solid reaction of the alloy with the steel substrate. This reaction is highly exothermic, and is controlled by the presence of silicon,[14, 20] some of which solidifies into a thin, barrier-type layer at the intermetallic/alloy interface. The alloy layer itself comprises of aluminium-rich dendrites (approximately 80 % by volume), together with interdendritic zinc-rich regions that contain needle-like particles of silicon.[13, 20] Macroscopically, the alloy coating surface is characterised by the formation of triangular-shaped areas known as spangles. Spangles can range in size from less than 0.5 mm (mini spangle) up to more that 3 mm (large spangle) in diameter, with the 'normal' size range being 1-3 mm.[13]

1.2.1.2 Uncoated Defects

Although numerous types of defects can occur in hot dip 55Al-43.4Zn-1.6Si coatings,[13, 21, 22] uncoated defects are one of the most prevalent. Uncoated defects are

discontinuities, or bare spots, in the hot dip metallic coating structure and appear as areas where either the intermetallic and/or the alloy layers are absent.[21-24] The size and distribution of uncoated defects across an area of alloy-coated steel can vary significantly and the defects can be anywhere from tens of nanometres (pinhole uncoated) through to centimetres (gross uncoated) in diameter (figure 1.7).[24, 25] They can occur in isolated patches over the surface of a coated steel sheet or they can cover the surface uniformly.

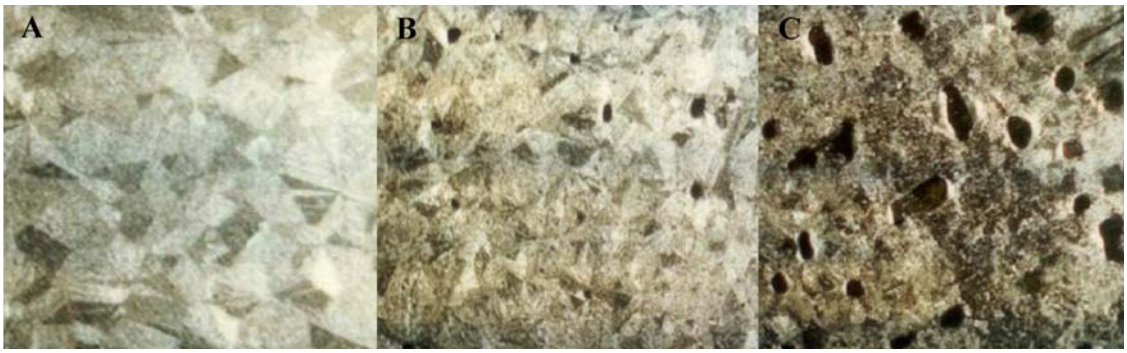

Figure 1.7 Photographs of a typical defect-free coating (A) together with coatings containing pinhole-uncoated (B) and gross-uncoated defects.[25]

The occurrence of uncoated defects has been associated with many factors, including incomplete pickling, insufficient pre-heating and reduction of oxides on the strip surface prior to hot dipping and the condensation and oxidation of zinc on the steel surface.[16, 21-24] However, the presence of oily residues on the steel strip surface has also been linked to uncoated defect formation.[22, 24, 26] It is suspected that changes to the steel surface chemistry, due to the persistence of oily residues after cold rolling and furnace cleaning, alter the steel surface energy and inhibit or preclude the alloy/steel reaction which is essential for intermetallic layer formation and 'wetting' of the steel surface by the molten alloy.[23, 24, 26, 27] The existence of uncoated defects compromises the appearance and anti-corrosion properties of coated steel products as well as the efficiency of downstream processes such as painting.[28] The level of uncoated defects present in alloy-

coated steel products is therefore highly indicative of coating quality.

The majority of research into uncoated defects has focused on the effects of steel surface oxidation and pre-heat temperature.[27, 29-34] Dionne et al.[27] studied the effect of pre-heat temperature and furnace conditions including dew point and hydrogen concentration on the formation of uncoated defects in galvanised hot rolled steels. Samples were prepared using a hot dip simulation apparatus and the resultant coatings were inspected both visually and using an image analysis system to determine the % uncoated area and the number of uncoated defects. Increasing the furnace hydrogen content from 5 % to 20 % dramatically improved coating quality, as did lowering the dew point from -5 ^{o}C to -30 ^{o}C. The effects of pre-heat temperature were dependent on steel composition, however higher pre-heat temperatures generally reduced the % uncoated area. These observations were attributed to lowering of the oxygen content of the furnace atmosphere. Scanning Electron Microscopy (SEM) coupled with Energy Dispersive Spectroscopy (EDS) analysis showed that the uncoated defect severity was related to the level of steel surface oxidation.

Ebrill et al.[29-34] have undertaken extensive research into the effect of steel substrate oxidation and pre-heat temperature on the dynamic wetting and coatability of low-carbon steel by both galvanising and Zincalume® alloys. A modified sessile drop apparatus was used to observe the wetting and spreading of the molten alloys onto steel surfaces. Increasing the substrate preheat temperature improved the degree of wetting, however the presence of oxides such as FeO and ZnO (formed by condensation and oxidation of zinc vapour from the coating bath) reduced wetting and spreading and increased the contact angle from $\theta \sim 25^{o}$ to $\theta >> 90^{o}$. Furthermore, hot dip simulation experiments enabled determination of the heat flux and resistance at the steel/alloy interface, showing that substrate oxidation increased the interfacial resistance and reduced the mass transfer of Fe and Al such that the wetting of the substrate was hindered. This corresponded to an increase in both the number and size of uncoated defects present in the resultant coating. Conversely, increasing the substrate pre-heat temperature to the coating bath temperature lowered the interfacial resistance, resulting

in improved wetting and coating quality. Williams et al.[23] expanded upon this research by constructing an experimental apparatus for the deposition of zinc vapour onto a steel substrate to study the effect of substrate exposure time and temperature on the mechanism of zinc vapour condensation.

Several other groups[21, 22] have undertaken general investigations into hot dip metallic coating defects and all have concluded that uncoated defects can arise from inadequate removal of oil residues from steel. However, the only research that has been specifically targeted towards studying the impact of rolling oils and their decomposition products on hot dip metallic coating quality has been conducted by Puente et al.[26] and Willem et al.[13]

Puente et al.[26] investigated the influence of three commercially available cold rolling oils on steel surface cleanliness, as determined by measuring changes in the surface brightness and carbon content. The impact of different cold rolling temperatures (100 ^{o}C and 150 ^{o}C) and surface cleaning processes (including alkaline and electrolytic degreasing) were also studied. Steel surface cleanliness was largely independent of the cleaning method employed, however rolling at lower temperature significantly reduced the amount of surface contamination, which was attributed to the formation of fewer oil degradation products. Despite this, there was no detailed analysis of the rolling oil or processing condition impact on the hot dip metallic coating quality and, more specifically, on uncoated defect formation.

Willem et al.[13] studied the impact of rolling oil residues present after cold rolling process on the formation of mini-spangle defects. Their results support the observations of Puente et al.;[26] increasing the temperature employed during the cold rolling process caused the occurrence of mini-spangles due to the formation of oil decomposition products such as metal carboxylates (soaps). Such soaps could not be effectively removed by conventional electrocleaning methods so that a more stringent cleaning process was devised to minimise oil deposits. It was noted that the soaps were ‘burned off’ in a pre-heating furnace, a process which was confirmed by hot dipping simulation experiments during which that steel substrate was treated in air at a series of different temperatures. Heating the steel substrate to 450 ^{o}C for 5 s was sufficient to prevent mini-

spangle defects. However, no observations regarding uncoated defects were made.

In summary, whilst the impact of furnace cleaning parameters, such as pre-heat temperature and gas atmosphere composition, on the formation of uncoated defects in hot dip metallic coatings has been studied in detail, no comprehensive study targeting the relationship between rolling oil composition, the detection and chemical nature of oil decomposition deposits remaining after furnace cleaning and uncoated defect formation has been performed. Furthermore, the majority of investigations have focussed on galvanized, as opposed to Zincalume®, coatings.

1.2.2 Oil Residue Formation

1.2.2.1 Cold Rolling Oils

In 1998, Keyser[35] identified that the two key contaminants present on the steel surface after cold rolling are iron, in the form of iron fines, and oil in the form of soaps, contaminants ('tramp' oils) and residual oil from the rolling process. Excessive iron fines result from high levels of wear during the rolling process.[35, 36] Not only do the fines accelerate the rate of rolling oil oxidation; their presence can cause hot dip metallic coating defects.[35] Typical tests for iron include the 'tape test', where iron particles on the steel surface are removed using a piece of tape; the more reflective the tape, the more iron is on the surface.[35] This type of test is rudimentary and qualitative in nature, and it does not account for iron present in other than particulate forms. A more quantitative method for assessing iron levels involves ultrasonic solvent cleaning of the steel surface followed by filtration, acid digestion and Atomic Absorption Spectroscopy (AAS) analysis of particulate matter.[12, 35] Iron soaps are also determined by evaporating solvent from the filtrate, digesting the resultant residue and testing by AAS.[12]

The composition of the rolling oil remaining on the steel surface following the cold rolling process is affected by three primary variables; the presence of 'tramp' oil contaminants such as hydraulic and bearing oils leaked from the rolling mill, oil decomposition during storage and re-circulation and oil decomposition during the rolling process itself. Tramp oils cause problems during all stages of the coated sheet metal

production process. They result in decreased lubrication performance during cold rolling and they have been shown to cause the formation of high surface carbon levels following the batch annealing process.[35, 36] Re-circulation and storage of rolling oil emulsion at temperature leads to the evolution of acidic and soap-like oil decomposition products by oil oxidation and hydrolysis.[12] The build up of these products is controlled by routinely analysing the oil emulsion properties including the Total Acid Number (TAN) or Free Fatty Acid (FFA) content, the Emulsion Stability Index (ESI) and the oil droplet particle size and distribution.[5, 12, 35, 37] Analogous decomposition products exist in the residual rolling oil layer present on the steel surface following the cold rolling process[5, 12, 37] and the possibility of further oil oxidation/decomposition product build up exists during the time when the steel coils are left to cool prior to metal coating.[17]

Chromatographic and mass spectrometric techniques have been used to assess solvent-extracted rolling oil residues,[37-41] however interpretation of the results is complicated. The complex makeup of rolling oils renders qualitative and/or quantitative identification of individual rolling oil constituents difficult and any meaningful interpretation of chemical changes occurring in these constituents as a result of the cold rolling process is virtually impossible. Furthermore, wet chemical methods increase the risk of sample contamination. Derivatisation of extracted oil components is almost always required and it is questionable as to whether chemisorbed species are completely removed from the steel surface.[41, 42]

Surface-orientated Fourier Transform Infrared Spectroscopic (FTIR) techniques such as Attenuated Total Reflectance (ATR) and Infrared Reflection-Absorption Spectroscopy (IRRAS) have emerged as a more direct method for analysing rolling oil-derived steel surface residues.[40, 41, 43-45] A range of inorganic as well as organic components are detectable and quantitative as well as qualitative analysis can be achieved.[12] Tamai and Sumimoto[43] simulated the process of oil-burn during cold rolling by clamping neat rolling oil-coated and rolling oil emulsion-coated steel sheets together, treating them in an air oven at ~ 90 ^{o}C for 20 hrs, washing the steel surface to remove non-adhered material and subsequently analysing the surface by ATR and contact angle

measurements. All samples treated with neat or emulsified rolling oil gave higher contact angles than the steel control sample, implying there was good adhesion of the organic residue to the steel surface. The ATR results confirmed that the emulsion-treated oil samples reacted with the steel surface to form iron soaps, however soaps were not detected on the neat rolling oil-treated samples.

FTIR methods have also been developed to analyse the composition of rolling oil formulations and emulsions; Cole et al.[46] used ATR to quantify the amount of oil present in rolling oil emulsion, Fujioka and Tanikawa[37] combined infrared detection with High Performance Liquid Chromatography (HPLC) to isolate five carbonyl-based rolling oil components and Chopra et al.[47] identified ten different known ingredients present in a rolling oil formulation using multi-component analysis, although they were unable to identify unknown ingredients.

Despite the amount of research undertaken into effect of cold rolling on rolling oil decomposition, it is the composition of the steel surface following the furnace cleaning process which is critical to hot dip metallic coating quality. X-ray Photoelectron Spectroscopy (XPS), Auger Electron Spectroscopy (AES) and Glow-Discharge Spectroscopy (GDS) have been used extensively to study the efficiency of the furnace and electrochemical cleaning processes in removing rolling-oil derived residues.[28, 48-53] Payling et al.[48, 51] have undertaken research into the chemical composition of contaminants present on low-carbon steel sheet following the furnace cleaning process, however the bulk of their studies have focused on the detection and quantification of elements such as carbon. AES was used by Johannessen et al.[52] to profile and analyse defects in tinplate surfaces. The occurrence of de-wetting and non-wetting during electroplating was related to the presence of carbon stains or deposits on the tinplate surface and it was noted that these deposits could result from incomplete oil degreasing. Treverton and Thomas[50] used XPS to characterise the surface of annealed aluminium foil. Surfacial carbon deposits present on isolated areas of the surface adversely affected the adhesion of subsequent lacquer coatings. It was also noted that carbon residue binding energies were consistent with the presence of carboxyl-containing compounds

and mono-oxygen-substituted species such as aldehydes and alcohols. These findings were confirmed by subsequent analysis using Fast Atom Bombardment Mass Spectrometry (FABMS).

FABMS, together with other surface mass spectrometry techniques such as Secondary Ion Mass Spectrometry (SIMS) and Time-of-Flight Secondary Ion Mass Spectrometry (ToF-SIMS) can overcome the chemical structural limitations associated with x-ray and electron spectroscopic methods[42] and have been more commonly used for the analysis of metal surfaces[16, 42, 50, 54-56] and organic/inorganic coatings in general.[57-59] However, research employing these techniques has been focussed more on investigating the mechanism and the process of oil decomposition during lubrication as opposed to the chemical composition of surface contaminants remaining after annealing.[42, 54, 56]

Lafargue et al.[60] investigated the use of laser desorption/ablation techniques from a different perspective; their research was aimed at developing a laser desorption-based method for cleaning, as opposed to analysing, residues present on cold rolled and annealed steel sheet. The effect of wavelength, irradiance and the number of laser shots on the cleanliness and topography of the steel surface was investigated. By using different wavelengths of light, selective desorption of carbon- or iron-based contaminants was achieved although it was not possible to completely remove either of these residues.

Considerably less work has been undertaken to identify the processes undergone by rolling oils during furnace cleaning and the effect of factors such as oil composition and furnace atmosphere on the formation of thermally-stable oil residues. Pilon et al.[45] used grazing-angle FTIR to assess the chemical composition of industrially-annealed steel. A considerable amount of surface contamination in the form of hydrocarbons and silicones and/or silicates was detected, however as noted by Treverton and Thomas,[50] non-homogeneity in the contaminant layer coverage of the steel surface precluded accurate correlation between the amount of hydrocarbon-based residues determined by FTIR and the total amount of surface carbon determined by carbon analysis.

Fujioka and Tanikawa[37, 40] used FTIR and mass spectrometry to investigate the chemical

nature of oil-derived steel surface residues remaining after annealing cold rolled steel at 300 ^{o}C or 600 ^{o}C for 17-34 hrs under an HNX atmosphere. Oil residue samples were collected by abrading the steel surface with potassium bromide powder and extracting the oily residue into chloroform. The total amount of organic residue extracted from the steel annealed at 600 ^{o}C was 1.8 mg m^{-2} and the composition of this residue consisted of ester and long chain fatty acid decomposition products that were of higher molecular weight than the rolling oil base ester. A similar FTIR technique was employed by Shaw[49] to study reactions between rolling oil and a series of iron oxide/hydroxide powders over a two-week storage period at temperature and the effect of different degreasing and electrolytic pre-cleaning methods and batch annealing conditions on steel surface cleanliness.

Several industrial studies have been conducted to identify the chemical reactions and decomposition products evolved by rolling oil decomposition under batch annealing conditions.[61, 62] The chemical reactions (described in more detail in section 1.2.3.1) and volatile products evolved over different temperature ranges are summarised in table 1.2. Analogous investigations have not been performed in the presence of oxygen.

Table 1.2 Chemical reactions undergone by rolling oil over defined temperature ranges during the batch annealing process leading to the formation of volatile products.[61, 62]

Volatile Product	Process/Reaction	Temperature Range (^{o}C)
rolling oil	evaporation	RT-350
H_2O	evaporation, condensation reactions	RT-350
CO	decarboxylation	250-450
CO_2	decarboxylation	250-450
light hydrocarbons	thermal cracking	300-600
CH_4	thermal cracking	300-600
CO	residue combustion	600-700
CO_2	residue combustion	600-700
CH_4	residue reaction with H_2(g)	>700

Sech and Oleksiak[36] used Thermogravimetric Analysis (TGA) to study the effect of different rolling oil additives and contaminants under an HNX atmosphere in the presence and absence of 1 % w/w carbonyl iron powder. In the absence of iron, the fully-formulated rolling oil decomposed via a two-step process to leave essentially no residue at temperatures above 500 ^{o}C. The addition of carbonyl iron powder resulted in a more complex 3-step decomposition mechanism corresponding to an increase in residue levels, which was attributed to surface reactions between the oil and iron. Analysis of several different oil ingredients revealed that high molecular weight and high viscosity triglyceride, ester-based and tramp materials contributed significantly to residue levels due to their high volatilisation temperatures. The addition of sulfur-containing lubrication additives decreased residue levels from 1.4 % to below 0.6 %. This observation was ascribed to interactions between the sulfur and the iron inhibiting adhesion of the triglyceride and ester-based components. However, Sech and Oleksiak's study did not investigate the effect of an oxidising atmosphere on the oil decomposition and residue formation processes and failed to account for the presence of partially-oxidised oil species as a result of the cold rolling process.

Although Osten-Sacken et al.[63] employed simultaneous TGA and Differential Thermal Analysis (DTA) to study the decomposition and polymerisation reactions of carboxylate-based rolling fluids under both oxidising and inert conditions, such fluids are used in the cold rolling of aluminium as opposed to steel. Therefore, very little is known about the processes via which steel cold rolling oils decompose and form persistent residues under continuous annealing (oxidising) conditions.

1.2.2.2 Fuels and Other Lubricating Oils and Greases

In contrast to cold rolling oils, oxidative decomposition and residue formation in fuels and other lubricating oils and greases has been studied in great detail using a range of wet chemical and instrumental techniques. Various bulk and thin film oxidation methods have been employed including:

- Oxidation Characteristics of Inhibited Mineral Oils (TOST; ASTM D943-04a),

which measures the time taken for a 300 ml sample of oil to react with oxygen in the presence of water and an iron-copper catalyst;[64, 65]

- Oxidation Stability of Steam Turbine Oils by Rotating Pressure Vessel (RBOT/RPVOT; ASTM D2272-02), whereby the time taken for 30 g of oil to react with oxygen is determined in the presence of water and a copper catalyst inside a sealed vessel;[64, 66, 67]
- Thin Film Micro Oxidation (TFMO) test, where a small (25 μL) amount of oil is spread onto the surface of an activated high carbon steel catalyst and the amount of insoluble deposit formed by the oxidation process is determined gravimetrically;[68]
- Oxidation Stability of Lubricants by Thin Film Oxygen Uptake (TFOUT; ASTM D7098-06e1) which is used to evaluate automotive engine oil oxidative stability by simulating the conditions present in an operating engine;[10]
- Groupement Francais de Coordination (GFC) oxidation test, which is used to evaluate transmission oil oxidative stability and screen gear oils in Europe.[69]
- Thermal Oxidation Stability of Aviation Turbine Fuels (JFTOT; ASTM D3241-06), which rates the tendency of gas turbine fuels to deposit decomposition products,[70, 71]and
- a range of Institute of Petroleum (IP) Standards for studying oxidative stability.[67, 72]

Evaluation of test results is commonly performed using instrumental techniques such as GCMS, FTIR and NMR or by determining changes in sample viscosity and TAN. However, a major disadvantage of many of the above methods is the numerous steps involved and the considerable time (up to hundreds of hours) required to run experiments.[10, 73] Consequently, researchers have looked towards more rapid procedures based on thermal analysis techniques to study the oxidation and residue formation properties of lubricants.

TGA has commonly been employed to investigate the thermal decomposition of base oils used in the automotive industry,[10, 67, 74, 75] although the majority of studies have been performed under inert atmospheres. Gamlin et al.[10] evaluated the decomposition kinetics of a range of natural, semi-synthetic and synthetic engine base oils under nitrogen.

Isothermal, non-isothermal as well as modulated TGA techniques were employed. It was found that the decomposition temperature of the oils increased with increasing viscosity and that, comparing oils of similar viscosity, the thermal stability of the synthetic oils was superior to that of semi-synthetic and natural oils. Furthermore, the base oil decomposition process followed a first order kinetics up until 60 % oil mass loss, implying that volatilisation was not solely due to evaporation.

Similarly, the use of TGA in conjunction with GCMS to evaluate the effect of motor oil brand, grade and contamination upon oil thermal stability under nitrogen was reported by Sisk et al.[74] They ascertained that oxygen did not play a significant role in the pure oil decomposition mechanism and determined that the major decomposition reaction at 300 ^{o}C was hydrocarbon cracking. However, introducing a source of oxygen via contamination of the oils generated oxidative decomposition products such as aldehydes and carboxylic acids.

The most common thermal analysis technique employed to study the oxidative stability and residue forming tendency of lubricating oils and greases is Pressure Differential Scanning Calorimetry, or PDSC (refer to section 2.4.2 in Chapter 2 for a description of the technique). The high pressures employed in the PDSC technique suppress evaporation, enabling oxidation of volatile samples to be studied at high temperatures. The determination of oxidation induction time (OIT) from isothermal PDSC experiments has formed the basis of numerous investigations into the oxidative stability of greases[76, 77] and lubricating oils[10, 73, 78-81] as well as the effectiveness of anti-oxidants in preventing oxidative decomposition.[77, 78, 80, 81] PDSC OIT test results have shown good correlation with the more traditional oil oxidation test methods outlined above.[81] However, OIT measurements are primarily directed towards facilitating the development of lubricants with improved operating lifetimes; such measurements fail to evaluate the entire lubricant thermo-oxidative decomposition process and do not provide information of a lubricant's deposit-forming tendency. Although Adhvaryu et al.[68] and Gamlin et al.[10] used PDSC to study the oxidative decomposition of lubricant base oils under ramped heating conditions, their investigations once again focused on oil oxidative

stability, determined by the onset temperature of oxidation. Furthermore, Adhvaryu et al. noted that there was no linear correlation between the oxidation onset temperature and the formation of insoluble, high molecular weight oxy-polymeric deposits as measured by the TFMO test.

A second DSC-based technique used to study oxidative stability is Sealed Capsule DSC (SCDSC), which involves preparing the sample in a sealable DSC pan in a glove bag containing the atmosphere of choice (typically oxygen for oxidation experiments). As with PDSC, OIT results determined by SCDSC have been shown to correlate well with 'safe' lubricant operation data determined by more traditional methods.[64, 79, 82] However, limitations associated with the SCDSC technique render it unsuitable for evaluating lubricants under extreme oxidising or ramped heating conditions; lubricant/gas reactions are restricted by the initial amount of gas present in the sealed pan[82] and SCDSC experiments can only be performed under a limited range of heating rates to prevent sample evaporation from causing pressure build up inside the capsule.[64, 82]

Although the effect of different additives on deposit formation in lubricants has been studied in some detail (refer to section 1.2.3 below), few studies have employed PDSC or TGA techniques. Santos et al.[75] reported the use of TGA and DSC in conjunction with NMR, FTIR and rheological measurements to characterise the thermal degradation process of automotive lubricants and the effect of thermo-oxidative pre-treatment on the lubricant properties. Their results showed that lubricant oxidative degradation resulted in viscosity increases, which were due to the build up of high molecular weight polymerised products. TGA results revealed a three-step decomposition process in air, related to the volatilisation of low molecular weight products followed by hydrocarbon degradation and decomposition of high molecular weight hydrocarbons, whilst under nitrogen a single decomposition step consisting of a peak and a shoulder was observed. DSC analysis of the lubricants showed that two exothermic peaks were present at high temperature in air, indicating that the hydrocarbon decomposition reactions observed by TGA were due to combustion. No exothermic peaks were observed under nitrogen. Thermo-oxidative degradation pre-treatment of the lubricants reduced the onset

temperature of decomposition and therefore the thermal stability of the samples.

Given the link between lubricant oxidation and the formation of thermally-stable high molecular weight decomposition deposits, the activity of different metals in catalysing the oxidation process is of critical importance and has been studied by several groups.[65, 72] However, no comprehensive investigation linking lubricant composition and oxidation conditions to the process of oxidative decomposition and residue formation has been performed.

1.2.2.3 The PDSC 2-Peak Method

The most relevant PDSC study into the residue-forming properties of lubricants is that undertaken by Zhang et al.,[83, 84] who in 1992 described the development of a new PDSC-based test for evaluating the deposit-forming tendencies of diesel engine oils. The motivation behind the establishment of this test was to enable rapid, laboratory-based oil screening prior to the evaluation of oil performance using costly, time-consuming engine tests. The test conditions were designed to simulate the environment found in an engine whilst optimising reproducibility and discrimination between oil samples. Underpinning the test method was the assumption that the deposit formation process occurs according to scheme 1.3.

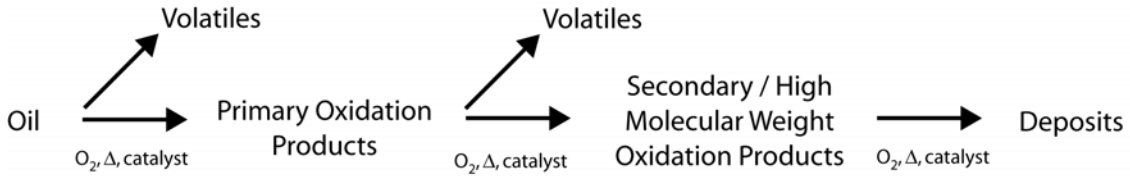

Scheme 1.3 Simplified model for oil oxidation.[83, 84]

The model shown in scheme 1.3 has been shown to accurately predict the process of oil oxidation providing there are no oxygen diffusion limitations.[83-85] Oil oxidation leads to the formation of primary oxidation products which, upon further heating, form high

molecular weight secondary oxidation products and eventually varnish-like deposits. The reactions leading to deposit formation compete with oil evaporation and the volatilisation of primary oxidation products such that appropriate PDSC test conditions must be selected to minimise volatility and obtain repeatable oxidation results.

The optimised PDSC test procedure reported by Zhang et al.[84] involved placing a thin (0.7-0.8 mg) film of oil, to ensure adequate oxygen diffusion, onto the surface of a specially-designed steel pan sealed with a lid containing a 0.65 mm diameter hole. The pan was then placed into the PDSC cell and the test was conducted over the temperature range 50-550 ^{o}C using a heating rate of 2 ^{o}C min^{-1} at temperatures below 340 ^{o}C and 10 ^{o}C min^{-1} above 340 ^{o}C, an oxygen pressure of 689 kPa and a gas flow rate of 20 ml min^{-1}. Two net exothermic peaks were observed in the resultant oil thermograms; a primary oxidation peak, representing the total energy involved in oil oxidation reactions, evaporation and polymerisation, and a secondary oxidation peak, attributed to the combustion of high molecular weight material and deposits remaining after primary oxidation. These peaks were referred to as the A and B peaks respectively. Zhang et al. proposed that the ratio of the B peak to the A peak, the % B/A ratio, could be used as an indirect measurement of the amount of deposit formed by an oil under the specific oxidation environment outlined above. The % B/A ratios determined for a series of engine oils were sufficiently different to enable oils to be distinguished and were found to correlate well with engine test results.

In 1998, Quaker Chemical developed an analogous test to measure the residue forming-tendencies of rolling oil formulations. A study was undertaken in conjunction with BlueScope Steel® (then BHP Steel) in which the PDSC 2-peak method was utilised to investigate the relationship between rolling oil residue formation and the occurrence of uncoated defects in Zincalume® coated steel at the Springhill Plant.[25] The results of this study showed that there was generally a good correlation between the % B/A ratios determined for different rolling oils and uncoated defect severity; oils with a % B/A ratio of less than 7 % produced defect-free coatings. In addition to this, the % B/A ratio was generally found to increase with the concentration of sulfurised lubrication additives

in the rolling oil, suggesting that the formation of thermally stable sulfur-based deposits could be a major source of coating problems. The presence of contaminant tramp oils such as Morgoil and hydraulic fluid in the rolling oil was also found to increase the % B/A ratio. However, the technique produced ambiguous results for several rolling oil formulations; one oil gave a high % B/A ratio but did not produce uncoated defects. Furthermore, the test reproducibility was poor and some oils produced % B/A ratio results that varied between 2 and 13 %. These observations highlight the need to optimise the PDSC 2-peak test conditions to enable assessment of rolling oil residue formation properties. In addition, the requirement for complementary methods of rolling oil residue analysis is evident given that the PDSC 2-peak technique does not provide information on the chemical nature of rolling oil residues present at any stage during the oxidation process, or the dependence of residue formation on oil formulation composition.

1.2.3 Decomposition and Oxidation of Specific Oil Constituents

As previously noted, the rolling oils employed during the steel cold rolling process are complex formulations containing numerous different ingredients. The analysis and characterisation of such mixtures and their thermal decomposition reactions is therefore complicated, and these complications are intensified by the fact that the majority of the ingredients used in rolling oil formulations are derived from natural products. In order to interpret the chemical processes that occur during the thermal decomposition of a complete rolling oil formulation, it is necessary to understand the thermal behaviour of the individual rolling oil components. It is also essential, in determining the relationship between rolling oil chemistry, the formation of thermally stable oil decomposition residues and hot dip metallic coating quality, to consider the chemical differences between rolling oils that potentially give rise to uncoated defects. Three key classes of rolling oil ingredients which have been associated with the deposit formation are base esters (including triglycerides), sulfurised EP additives and phosphorus-based lubrication additives. The proceeding section reviews the chemical processes via which

each of these classes of ingredients decompose to form thermally-stable deposits.

1.2.3.1 Triglycerides and Base Esters

One of the predominant differences between rolling oil formulations is the chemical structure of the base ester. Base esters typically constitute between 20 and 90 % w/w of a rolling oil formulation[12] and are the foundation from which rolling oils are blended. The chemical composition of a base ester is defined by cold rolling mill lubrication requirements, however blends incorporating naturally-occurring triglycerides (from sources such as coconut oil and tallow) in conjunction with synthetic di- and tri-ester derivatives are common.[9, 86] Synthetic ester derivatives are produced via a trans-esterification process whereby the desired polyfunctional alcohol is esterified with triglyceride fatty acids (scheme 1.4).[87] The reaction is usually terminated such that the resultant ester contains a small proportion of free fatty acids and hydroxyl groups.

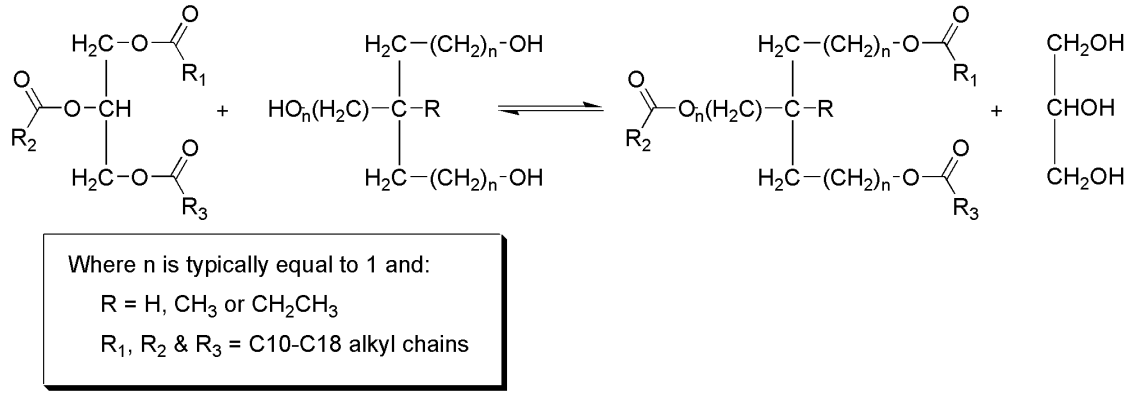

Scheme 1.4 Representation of a trans-esterification reaction between a triglyceride and a tri-functional alcohol yielding glycerol and a new ester.

Esters produced via scheme 1.4 are often termed ‘semi-synthetic’ as they possess the fatty acid distribution of a naturally-occurring triglyceride with a synthetic alcohol component. In contrast, ‘fully-synthetic’ base esters derive both their alcoholic and fatty acid components from synthetic sources. The primary advantage of semi- and fully-

synthetic base esters over their triglyceride counterparts is that they exhibit improved hydrolytic, thermal and oxidative stability,[10, 11, 86] which are essential properties for ensuring lubrication performance within the severe conditions employed during cold rolling.

The chemical structure and distribution of the fatty acid alkyl chains obtained from different triglyceride sources vary significantly, and are determinative of the above properties as well as physical state and lubricity.[87] Variations can be found in fatty acid carbon chain length, degree of unsaturation and the presence of unique functionalities such as hydroxyl (OH) groups. Table 1.3 illustrates some of these variations by summarising the typical fatty acid compositions of several common vegetable- and animal-derived triglycerides.

The majority of triglycerides and semi-/fully-synthetic esters used in rolling oils contain three reactive functionalities; the ester linkage, OH groups on the ester head group and/or in the fatty acid alkyl chain, and carbon-carbon double bonds (C=C) present in the fatty acid alkyl chain.[9, 87] The primary reactions of the ester linkage are hydrolysis (scheme 1.5A), saponification (scheme 1.5B) and trans-esterification (scheme 1.4).

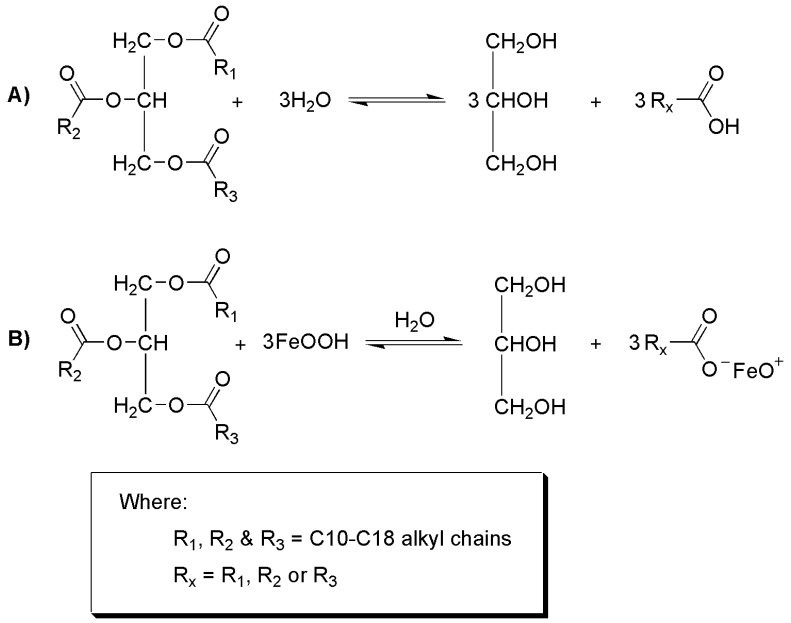

Scheme 1.5 Hydrolysis (A) and saponification (B) reactions of triglycerides.

Table 1.3 Typical fatty acid compositions of several common vegetable- and animal-derived triglycerides. The percentage by mass of poly-unsaturated, mono-unsaturated and saturated fatty acid chains is included.[87]

Triglyceride	Fatty Acid (% by mass)													% polyunsaturates (w/w)	% monounsaturates (w/w)	% saturates (w/w)
	Caprylic, C8:0	Capric, C10:0	Lauric, C12:0	Myristic, C14:0	Palmitic, C16:0	Palmitoleic, C16:1	Stearic, C18:0	Oleic, C18:1	Linoleic, C18:2	Linolenic, C18:3	Arachidic, C20:0	Behenic, C22:0	Ricinoleic, C18:1(OH)			
Coconut Oil	6.0	5.0	43.8	19.0	11.6	0.1	5.1	7.4	1.8					1.5	6.5	92
Palm Oil			0.3	1.1	45.1	0.1	4.7	38.5	9.4	0.3	0.2			9.7	39	51
Cottonseed Oil				0.9	24.7	0.7	2.3	17.6	53.3	0.3	0.1			54	18	28
Sesame Oil					9.9	0.3	5.2	41.2	43.2	0.2				43	42	15
Safflower Oil				0.1	6.5		2.4	13.1	77.7		0.2			78	13	9.2
Canola Oil					3.9	0.2	1.9	64.1	18.7	9.2	0.6	0.2		28	64	6.6
Castor Oil					0.9	0.2	1.2	3.3	3.7	0.2			89	3.9	89	2.1
Lard Oil			0.1	1.5	24.8	3.1	12.3	45.1	9.9	0.1	0.2			48	10	39
Beef Tallow		0.1	0.1	3.3	25.5	3.4	21.6	38.7	2.2	0.6	0.1			42	2.8	51

Saponification is of particular importance in the cold rolling industry; as noted above, metal soaps have been identified as one of the key contaminants left on the steel surface following the cold rolling process.[35, 49] The structure and properties of metal soaps have received considerable attention over the past twenty years due to their importance in a broad range of industries.[88, 89] The thermal decomposition of synthetic, short-chain (≤ C18) soaps is known to involve the formation of ketones, metal oxides and carbon dioxide (scheme 1.6) and is essentially complete between 460-530 ^{o}C.[89-92] Comparatively little academic focus has been directed towards studying the metal soaps formed during the cold rolling process[49] such that the chemical nature, process of thermal decomposition and impact of these soaps on downstream steel surface treatments is poorly understood.

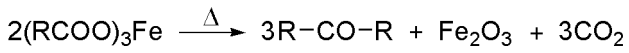

Scheme 1.6 Thermal decomposition of an iron(III) soap to form a ketone, iron(III) oxide and carbon dioxide.[91]

Hydrolysis is also relevant to the cold rolling process as the rolling oil is applied as an aqueous emulsion. Re-circulation and storage of the rolling oil emulsion at above-ambient temperatures has been shown to accelerate ester hydrolysis and cause lubricant degradation over time.[12] The build-up of excessive amounts of mono- and di-esters and fatty acids within the rolling oil can be detrimental to lubrication performance and result in excessive saponification.[9, 12]

OH groups present on the ester head group and/or in the fatty acid alkyl chains can undergo condensation reactions to form polymers according to scheme 1.7.[87] Given the high pressures applied during the cold rolling process and the creation of fresh metal surfaces, adsorption of ester head group OH functionalities to the steel surface (as per scheme 1.5) is likely to occur preferentially to the condensation reactions shown in scheme 1.7A. Furthermore, according to table 1.3, OH groups are absent in the alkyl chains of the majority of naturally-occurring triglycerides (and hence in their semi-

synthetic derivatives) such that condensation reactions in the alkyl portion of base esters (scheme 1.7B) are minimal. Castor oil is unique in that ~ 89 % of its fatty acid chains comprise of ricinoleic acid. Condensation reactions of castor oil's OH groups are exploited within the coatings and materials industries,[93-95] however the use of castor oil in the cold rolling industry has not been documented.

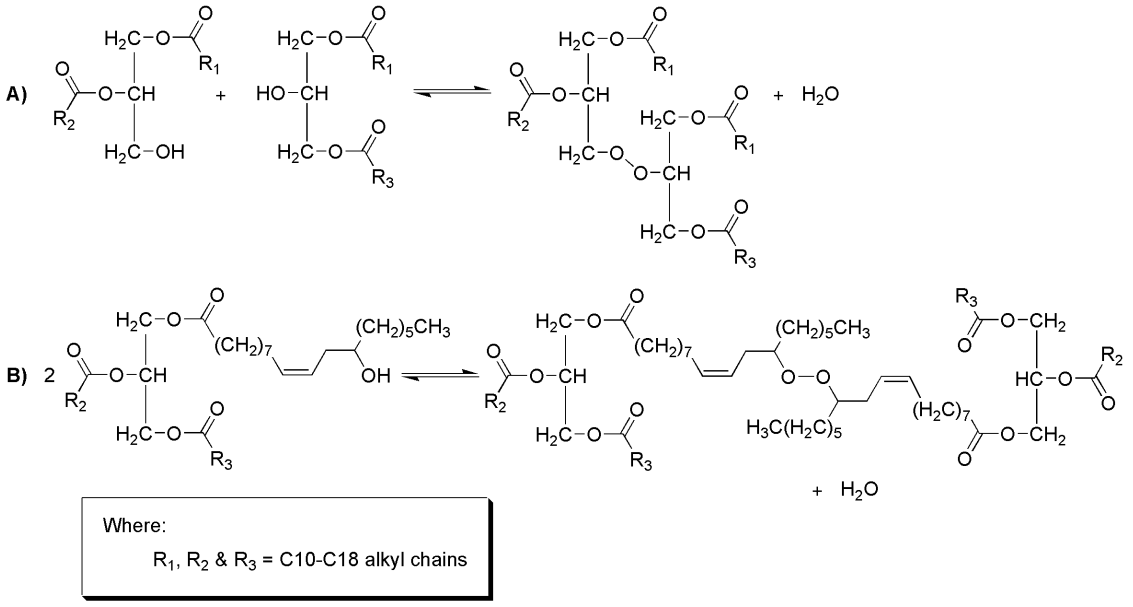

Scheme 1.7 Condensation reactions of hydroxyl groups present on the triglyceride ester head group (A) or within the alkyl chain (B).

The presence of C=C bonds in ester alkyl chains enables both addition reactions (scheme 1.8) and oxidation to occur.[87] The addition reactions of C=C bonds will be considered further below in the context of oxidation, however addition of hydrogen gas to C=C bonds (hydrogenation) is relevant to the removal of residual cold rolling oil during the batch annealing process.

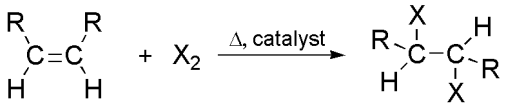

Scheme 1.8 Addition reaction between a C=C bond and a diatomic molecule.

C=C bond oxidation in unsaturated esters occurs via a free-radical, autocatalytic mechanism[87, 96, 97] and has been studied in great detail due to its importance in the food and lubricant industries. The unsaturated ester oxidation process is widely accepted as involving seven main processes including induction, oxidation initiation, hydroperoxide formation, hydroperoxide decomposition, crosslinking/polymerisation, radical recombination and radical decomposition (secondary oxidation). These processes are described in detail below.

The induction period commonly observed during triglyceride oxidation results from the presence of naturally-occurring phenolic anti-oxidants such as tocopherols, tocotrienols and a range of triglyceride-specific compounds.[87, 98, 99] With respect to cold rolling oils, the high degree of processing employed in the preparation of triglycerides and semi-synthetic esters minimises the concentration of natural anti-oxidants.

Oxidation initiation involves hydrogen abstraction from the ester alkyl chain (R-H) by an initiating species, such as a metal complex or peroxide radical ($X^{\bullet}$), to form an alkyl radical ($R^{\bullet}$; scheme 1.9).[96, 97, 100, 101]

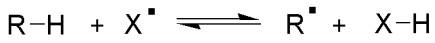

Scheme 1.9 Hydrogen abstraction from an ester alkyl chain by an initiating species to form an alkyl radical during oxidation initiation.

Hydrogen abstraction occurs preferentially from allylic positions in unsaturated alkyl chains and the subsequent reaction of $R^{\bullet}$ with molecular oxygen to form peroxide radicals ($ROO^{\bullet}$) occurs rapidly (scheme 1.10).

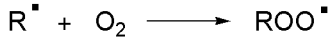

Scheme 1.10 Reaction between an alkyl radical and molecular oxygen to form a peroxide.

The initiation process can be accelerated by irradiation to UV light, through the addition of radical-generating species such as peroxides, and, importantly in the case of cold

rolling, through the use of metal-based catalysts and by the application of heat.[72, 87] An alternative pathway for oxidation initiation involves the direct addition of singlet-state oxygen to C=C bonds via an ene addition reaction, however the use of a photo-sensitising agent and exposure to UV light are required.[96, 97, 99]

Hydroperoxide formation is a radical propagation reaction whereby peroxide radicals abstract hydrogen from the ester alkyl chain (scheme 1.11);

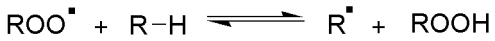

Scheme 1.11 Peroxide radical hydrogen abstraction from an ester alkyl chain to form an hydroperoxide.

Hydroperoxide decomposition subsequently generates a range of alkyl ($R^{\bullet}$) and oxygenated ($^{\bullet}OH$, $RO^{\bullet}$, $ROO^{\bullet}$) radical species (schemes 1.12A-1.12B), which can participate in hydrogen abstraction reactions according to scheme 1.11.

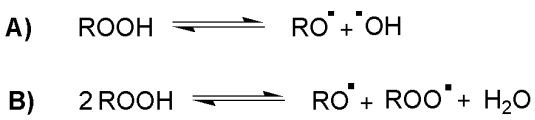

Scheme 1.12 Hydroperoxide decomposition pathways including dissociation (A) and disproportionation (B).

As noted with respect to oxidation initiation, metals such as iron oxides can catalyse hydroperoxide decomposition via redox reactions (schemes 1.13A-1.13C).[65, 72]

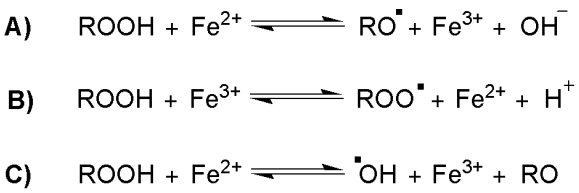

Scheme 1.13 Redox reactions between iron oxides and hydroperoxides resulting in the catalysis of hydroperoxide decomposition.

Solubility plays an important role in metal catalytic activity; soluble metal particles significantly increase the rate of hydroperoxide decomposition reactions.[65, 72] During the steel cold rolling process, the availability of iron fines in addition to iron oxides on the steel surface provides a highly favourable environment for oil oxidation.

Crosslinking/polymerisation is a radical propagation reaction involving the addition of radicals to C=C bonds in the ester alkyl chain (scheme 1.14).

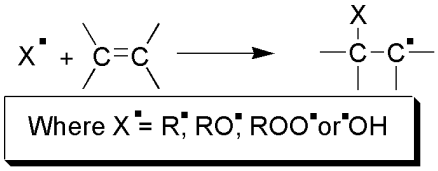

Scheme 1.14 Addition of alkyl or oxygenated radicals to C=C bonds to form branched/networked material.

The addition of radicals to C=C bonds leads to the formation of high molecular weight branched and/or networked material. In triglycerides and base esters, propagation of the resultant radicals can involve the formation of inter- and/or intra-molecular crosslinks between alkyl chains such that the formation of networked material is almost inevitable. Although the build up of high molecular weight deposits in oxidised lubricants has been shown to lower the coefficient of friction and reduce wear under boundary lubrication conditions as a result of the increased viscosity of the polymer film,[11] such deposits are likely to be detrimental to the hot dip metallic coating process; as noted previously, residual organic matter on the steel surface has been associated with poor wetting by the molten alloy and the formation of uncoated defects;

The oxidation chain reaction is terminated by radical recombination, whereby high molecular weight material containing C-C, C-O-C and C-O-O-C linkages is formed (schemes 1.15A-1.15I; the reaction shown in scheme 1.12A may also occur).

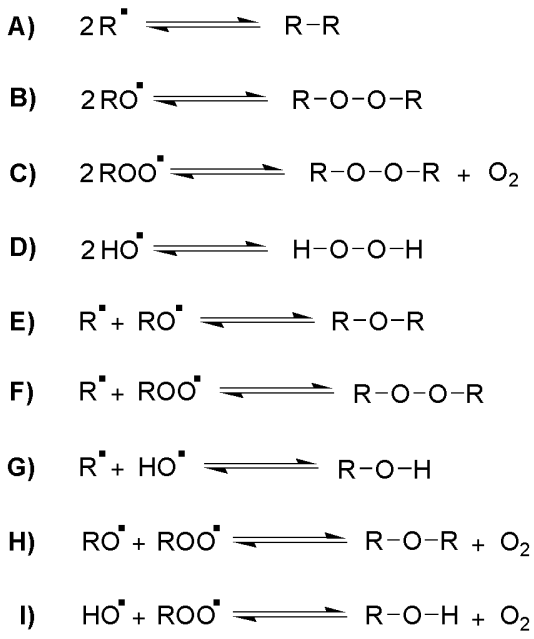

Scheme 1.15 Homogeneous (A-D) and heterogeneous (E-I) radical recombination reactions.

Finally, radical decomposition/secondary oxidation reactions such as β-scission and Russell termination,[99, 100, 102-107] which compete with hydroperoxide formation, polymerisation and radical recombination reactions, lead to the evolution of volatile and non-volatile low molecular weight products such as alkanes, aldehydes, carboxylic acids, ketones and alcohols (schemes 1.16A-1.16B).

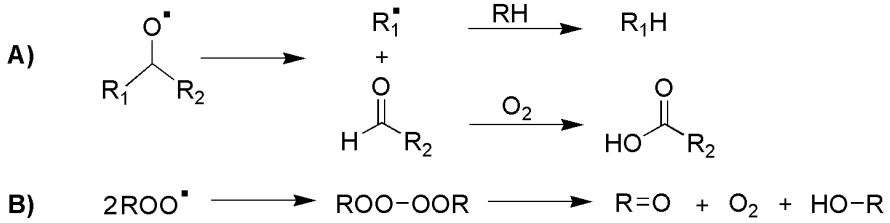

Scheme 1.16 β-scission (A) and Russell termination (B) reactions of oxygenated radical species.

At higher temperatures esters undergo decarboxylation, thermal cracking and combustion. As noted in table 1.2, rolling oil decarboxylation occurs between 250-450

^{o}C (scheme 1.17).[61, 62] Cracking reactions occur at slightly higher temperatures and evolve short-chain, gaseous hydrocarbons and high molecular weight carbonaceous deposits (schemes 1.18A-1.18E; the radicals formed can also participate in hydrogen abstraction via scheme 1.11).[61, 62, 108]

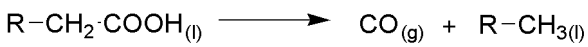

Scheme 1.17 Fatty acid decarboxylation, producing carbon monoxide and hydrocarbon.

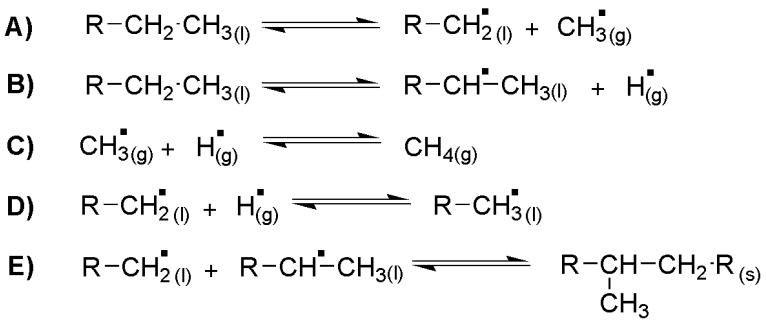

Scheme 1.18 Thermal cracking reactions (A & B) to form methane (C) and residue (D & E).

Combustion leads to the removal of such deposits via the formation of carbon dioxide and water (scheme 1.19).

Scheme 1.19 Complete hydrocarbon combustion producing carbon dioxide and water.

Finally, during the cold rolled steel annealing process, further reactions between residual carbonaceous products, gaseous products, the annealing atmosphere and the steel surface may occur (schemes 1.20A-1.20).

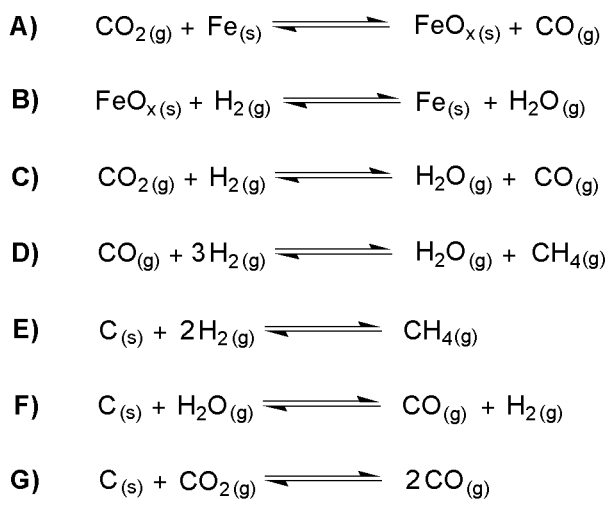

Scheme 1.20 High temperature reactions between the steel surface, residual carbonaceous deposits, gaseous decomposition products and gas present in the annealing atmosphere. Reactions B-E are particularly relevant to the batch annealing process.

The importance of triglycerides in the food industry has ensured that the thermo-oxidative stability of naturally-occurring esters has received a great deal of attention. DSC (including SCDSC and PDSC) and TGA techniques have been used extensively to evaluate the mechanism and kinetics of triglyceride oxidation and decomposition[11, 85, 101, 109-114] and the results obtained have been shown to correlate well with traditional methods for oil oxidation analysis.[11, 110, 111, 114] Numerous PDSC investigations have confirmed the autocatalytic nature of the triglyceride oxidation process.[113, 115] However, as noted above with respect to the lubricant industry, the majority of these studies are performed under isothermal conditions and are directed towards evaluating triglyceride resistance (with and without the addition of anti-oxidant packages) towards oxidation.[85, 110-113] Comparatively little research has been done to relate the chemical characteristics of triglycerides, such as fatty acid saturation levels, chain length and structure (such as the presence of OH functionality), to the mechanisms involved in their decomposition under continuous heating conditions[85] or over extensive temperature ranges.[116, 117] Although the majority of such research has been performed by TGA, no studies have been reported on the relationship between triglyceride chemical properties and the level

of residue remaining following triglyceride thermal decomposition.

Dweck and Sampaio[116] studied the thermal decomposition of canola, sunflower, corn, olive and soybean oils in air by simultaneous TGA and DTA between room temperature and 700 ^{o}C in order to compare oil thermal stability and calorific content. Decomposition of all the oils proceeded via four main steps. The first step was not ascribed to any particular chemical process, however it was noted that there was a relationship between the onset temperature of mass loss and the carbon chain length of the fatty acid components of the oils. Similarly, variations in the second and third mass loss steps observed for the oils were reported to be due to differences in fatty acid composition. The fourth mass loss step was the only process to be chemically defined, and was attributed to the removal of residual carbonaceous material. It was also hypothesised that the composition of this residue was dependent on the preceding mass loss processes.

Santos et al.[117] evaluated the thermoanalytical, kinetic and rheological behaviour of a number of edible triglycerides in air. In contrast to the findings of Dweck and Samaio, the thermal decomposition of the oils was characterised by three mass loss events, which were attributed to the decomposition of polyunsaturated, monounsaturated and saturated fatty acids components. They noted that the onset of oil oxidation was typically indicated by a mass increase as a result of oxygen uptake. This mass increase was shortly followed by oil mass loss due to the formation of free radical oxidation products, such as peroxides and hydroperoxides, and the subsequent decomposition of these radicals into low molecular mass aldehydes and acids. Santos et al. also identified that the reactions of the monounsaturated esters during the second of the three mass loss events were likely to include polymerisation-type reactions leading to the formation of saturated products that were subsequently decomposed at higher temperatures during the final mass loss process. No persistent residues were detected at the maximum test temperature of 800 ^{o}C.

Coni et al.[98] have also studied the thermo-oxidative properties of vegetable oils, however their investigation was limited to the determination of the oxidation onset and endset temperatures and percentage mass gained by the sample during the oxygen uptake

process. They found that the onset temperature and initial mass gain were not only dependent on the chemical structure of the oil in question; the presence and concentration of naturally occurring anti-oxidants had a significant effect on oil oxidation.

TGA has also been used to study the thermal decomposition of long chain (n=10 to n=22) fatty acids and esters under non-oxidising conditions. Shen and Alexander[118] showed that the mass loss process for saturated fatty acids is a zero order reaction and is therefore due to evaporation, as opposed to thermal decomposition. The thermal decomposition of a variety of saturated and unsaturated long chain fatty acids, together with catfish and menhaden oils, was studied by Sathivel et al.[119] under nitrogen. They found that the thermal decomposition of the fatty acids was highly dependent upon both alkyl chain length and unsaturation. A comparison between C18:0, C18:1 and C18:2 fatty acids revealed that with increasing unsaturation, onset temperatures of mass loss were lowered whilst the proportion of mass lost at low (100-350 ^{o}C) temperatures was increased. The majority of the unsaturated fatty acids were completely decomposed by 400 ^{o}C, whereas complete decomposition of the saturated fatty acids was not achieved until 450 ^{o}C. TGA results for catfish and menhaden oil samples acquired at different stages throughout the oil refinement process showed that all oil samples were decomposed by 550 ^{o}C under nitrogen. The decomposition mechanism under this atmosphere was found to be non-oxidative; no oxygen uptake by the oils was observed. The only study to date on the thermal decomposition of long chain fatty acid methyl esters is reported by Dunn,[120] who used PDSC and TGA to investigate the decomposition of biodiesel in air.

1.2.3.2 Sulfurised Lubrication Additives

Sulfurised additives are regularly incorporated into steel cold rolling oil formulations to improve lubricant performance under EP conditions. Two of the most common classes of sulfurised EP additives are sulfurised hydrocarbons and sulfurised triglycerides. Representative chemical structures of these additives are shown in scheme 1.21.

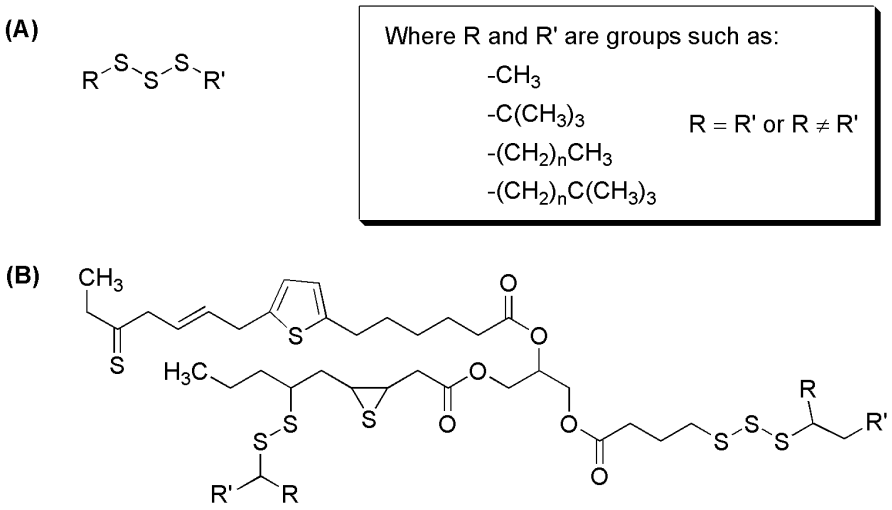

Scheme 1.21 Structural representation of typical sulfurised hydrocarbons (A) and sulfurised triglycerides (B).

Aside from the ester group in sulfurised triglycerides, the major reactive functional group present in sulfurised EP additives is the sulfide (S-S) linkage. The thermal decomposition reactions of sulfides are not only critical to their performance in lubrication applications; they are exploited in other areas of chemistry and engineering such as during the vulcanisation of rubber and in synthetic organic chemistry. A review of the literature in these areas, in addition to the literature concerning sulfurised lubrication additives, is therefore warranted as it can provide a fundamental insight into sulfur-compound thermal decomposition chemistry.

Sulfides can participate in two main types of reaction: thermal scission and oxidation. Scission of S-S bonds can occur either homolytically or heterolytically (scheme 1.22).[121] Homolytic scission is the typical sulfide decomposition pathway induced through the application of heat and leads to formation of alkylthiyl radicals ($RS^{\bullet}$). The ease with which homolytic S-S bond scission occurs, and therefore the reactivity of the sulfide, is dependent upon the S-S bond dissociation energy, which is in turn influenced by the length of the sulfur chain and nature of the adjoining alkyl groups. Table 1.4 summarises the S-S and C-S bond dissociation energies of some typical sulfides. The values given cover the range reported in the literature.[122-124]

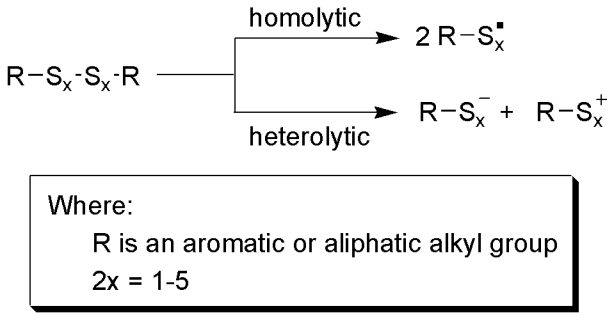

Scheme 1.22 Homolytic and heterolytic scission pathways for sulfides.

Table 1.4 C-S and S-S bond dissociation energies of some typical organic sulfides.[122-124]

Compound	Bond Dissociation Energy (kcal mol^{-1}) at 298 K	
	C-S	**S-S**
HSSH	-	63-67
CH_3SSH	60-67	64-67
CH_3SCH_3	73-77	-
CH_3SSCH_3	57-63	65-74
$C_3H_7SSC_3H_7$	53	62
$(CH_3)_3CSH$	68-79	-
$(CH_3)_3CSSC(CH_3)_3$	55-63	67-71
$C_6H_5SCH_3$	60-68 (CH_3-S)	-
$C_6H_5CH_2SCH_3$	59	-
$C_6H_5SSCH_3$	69-87 (C_6H_5-S); 55-66 (CH_3-S)	56-65
$C_6H_5SSC_6H_5$	73-87	49-61

It is evident that increasing the number of sulfur centres in the sulfide linkage lowers thermal stability, as does the presence of unequal, branched or longer alkyl chains adjacent to the sulfide linkage.[123, 125] C-S bond scission occurs preferentially to S-S bond

scission in branched/unequally-substituted sulfides and will be considered in further detail below.[125]

Alkylthiyl radicals formed via scheme 1.22 can participate in a vast array of competing processes/reactions including:

- isomerisation, involving hydrogen transfer to form thiolated alkyl radicals (scheme 1.23);[123]

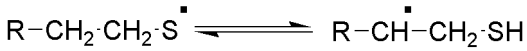

Scheme 1.23 Alkylthiyl radical isomerisation.

- hydrogen abstraction (from allylic or, at higher temperatures, saturated sites; scheme 1.24) producing alkyl radicals, which can participate in radical recombination or hydrogen abstraction reactions as outlined above,[123, 125, 126] and an alkanethiols, which decompose to generate a range of volatile products including hydrogen sulfide gas (H_2S) and hydrocarbons (schemes 1.25A-1.25D).[121, 123, 125-127]

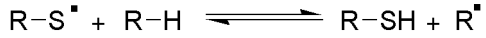

Scheme 1.24 Hydrogen abstraction by an alkylthiyl radical producing an alkyl radical and an alkanethiol.

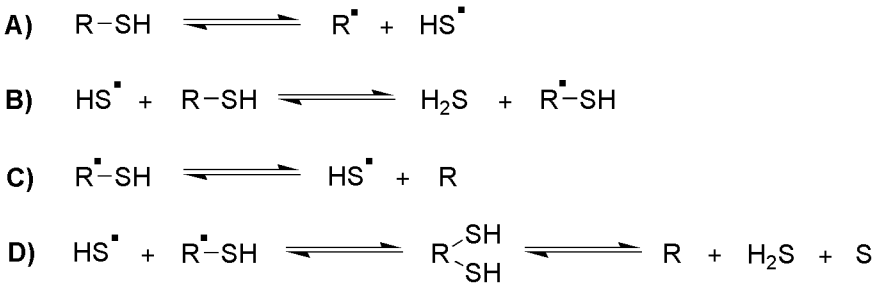

Scheme 1.25 Alkanethiol decomposition reactions generating H_2S and hydrocarbons.

- addition to C=C bonds to form high molecular weight branched and/or crosslinked products (scheme 1.26).[121] Such reactions are exploited during vulcanisation of rubber;

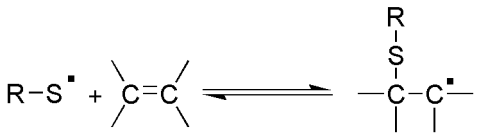

Scheme 1.26 Alkylthiyl radical addition to C=C bonds to form branched/networked material.

- recombination with other alkylthiyl/alkyl radicals formed by sulfurised additive decomposition, or with oxygenated radicals produced by C=C bond oxidation, to form a range of sulfurised hydrocarbons and oxygenated sulfurised hydrocarbons (schemes 1.27A-1.27B),[65, 121, 123, 125-127] and

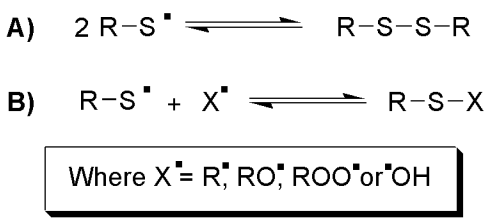

Scheme 1.27 Recombination reactions of alkylthiyl radicals with other alkylthiyl radicals (A) and with alkyl and oxygenated radicals (B).

- adhesion to metals to form thiolates (scheme 1.28A; note that this reaction can also occur for sulfides (scheme 1.28B) and alkanethiols (scheme 1.28C)).[128] C-S bond cleavage can occur to generate metal sulfides and/or the sulfur group oxidise according to scheme 1.31 below to form metal sulfates.

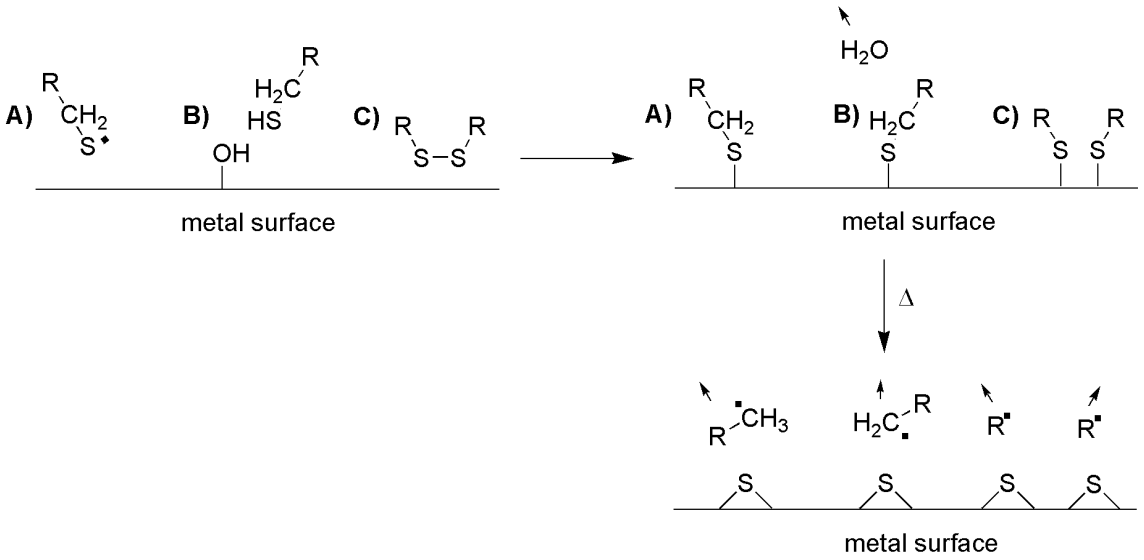

Scheme 1.28 Reaction between alkylthiyl radicals (A), alkanethiols (B) and sulfides (C) with a metal surface and subsequent C-S bond cleavage to form metal sulfides.

The thermal decomposition of sulfurised additives is therefore critical to EP lubrication performance as it promotes additive decomposition and adsorption to metal surfaces to create tribochemical films which prevent metal-to-metal contact, thus minimising friction, welding and wear.[128-131] Spectroscopic techniques have been extensively used to evaluate the effect of processing conditions (load, temperature) and sulfur additive chemical structure on the characteristics (chemical composition, thickness) of the resultant tribo-film.[128, 130-133] The use of X-ray Absorption Near Edge Structure spectroscopy (XANES) to study the properties of films generated using several sulfur-containing additives on steel was reported by Najman et al.[130, 131] In the first of these two studies,[131] the composition of films formed under thermo-oxidative and tribochemical conditions was compared. All three of the sulfurised additive examined (sulfurised isobutylene, zinc dithiocarbamate (ZDTC) and sulfurised ester) thermo-oxidatively decomposed at temperatures ≥ 100 ^{o}C to form iron sulfate ($FeSO_4$). In contrast, the films produced under EP and anti-wear (AW) conditions contained a mixture of products. Whilst the AW films, created using comparatively mild rubbing conditions, contained three forms of sulfur (small amounts of $FeSO_4$ and FeS with the dominant product being

FeS_2), the EP films contained only FeS and FeS_2, with FeS (formed by FeS_2 decomposition and/or direct reaction between sulfur and metallic iron) being the major product due to the presence of high interfacial temperatures.

The second of Najman et al.'s investigations reported the composition and properties of EP and AW films formed using binary mineral oil blends of sulfur and phosphorus-containing additives.[130] Although very little sulfur was detected in films formed under AW conditions (refer to discussion in section 1.2.3.3 below), the sulfur present in the EP films was once again predominantly comprised of FeS. FeS was also the major product detected by Lara et al.[128] in their study on the chemical composition and growth kinetics of EP films formed by dimethyl disulfide and by Komvopoulos et al.[132] for films formed on steel under boundary lubrication conditions at 32 ^{o}C and 100 ^{o}C. Komvopoulos et al. also noted that FeS was only formed on the wear track and that the concentration of FeS was greater at 100 ^{o}C than at 32 ^{o}C due to increased chemical reactivity between the sulfur additive and the steel surface. Interestingly, both FeS and oxidised forms of sulfur were detected on and off the wear track by a sulfur/phosphorus/metal deactivator additive blend. The purely thermal decomposition reactions between sulfurised olefin and iron oxides were studied by Riga et al.[134] by TGA (under an atmosphere of nitrogen) with XRD analysis of residues at 500 ^{o}C and 1000 ^{o}C showing the presence of FeS and Fe_3S_4 respectively.

Given the reactivity of sulfur lubrication additives with metal surfaces, it is perhaps not surprising that the presence of sulfur-containing compounds in fuels and lubricating oils has also been associated with the formation of sludge-like deposits.[71, 126, 133] Fabuss et al.[126] investigated the effect of typical organosulfur contaminants, including thiophene, benzenethiol, di-*tert*-butyl disulfide, diphenyl sulfide and diphenyl disulfide, on the thermal decomposition rate of several saturated pure hydrocarbons. It was found that the nature of the hydrocarbon (straight-chain, branched or cyclic) had a greater effect on the rate of decomposition than the chemical nature of the sulfur compound. However, the sulfur contaminants generally accelerated the rate of decomposition of branched hydrocarbons and inhibited the decomposition of straight-chained hydrocarbons. Fabuss et al. rationalised this observation by deducing that the majority of the sulfur compounds

studied would decompose at lower temperatures than the hydrocarbons, forming organosulfur radicals ($RS^{\bullet}$; refer to scheme 1.22 above) which could participate in hydrogen abstraction (scheme 1.24) or recombination reactions (schemes 1.27A-1.27B). If hydrogen abstraction by $RS^{\bullet}$ occurred preferentially to radical recombination, the rate of hydrocarbon decomposition would be accelerated and vice versa.

C-S bond scission generally requires more energy to occur than S-S bond scission, especially in sulfides containing short S-S chains/homogeneous aliphatic alkyl substitution, and therefore tends to occur at higher temperatures.[123, 125, 127] Schemes 1.29A-1.29F illustrate the C-S scission reactions undergone by a typical sulfurised hydrocarbon, diisopropyl disulfide, resulting in the formation of propene and H_2S.

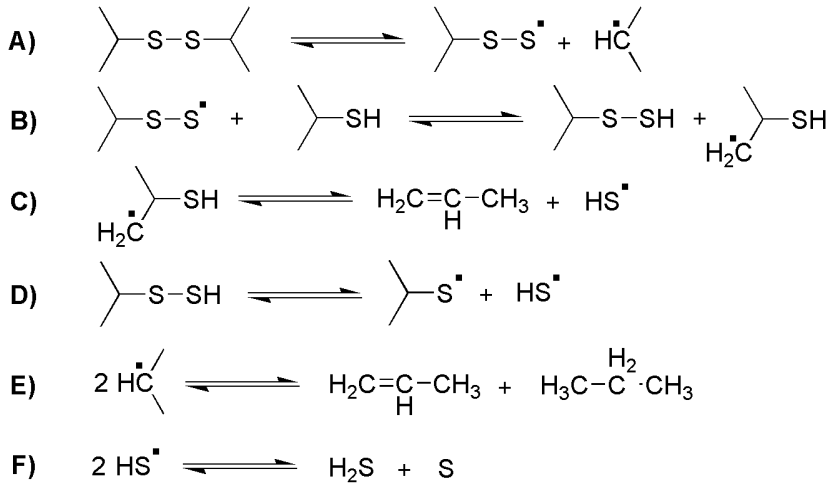

Scheme 1.29 C-S bond scission shown for diisopropyl disulfide (A) and reaction with 2-propanethiol (B) formed according to scheme 1.24, leading to the evolution of propene (C & E) and H_2S (D & F).

C-S scission reactions were used by Sundarrajan et al.[135] to rationalise the products detected by pyrolysis-GCMS analysis of several saturated and unsaturated polysulfide polymers. The resultant alkylthiyl radicals participated in backbiting reactions, yielding a range of hydrocarbon-based and sulfur-containing aromatic and cyclised compounds such as benzenes and thiophenes.

Other sulfur-containing functional groups, such as thiophenes and thiiranes, are also

present in sulfurised triglycerides. The high thermally stability of thiophenes (> 500 ^{o}C) is documented in the literature,[126] however thiiranes are known to decompose at comparatively low temperatures (200-250 ^{o}C) via the formation of an excited transition state to form ethylene and elemental sulfur (scheme 1.30).[125]

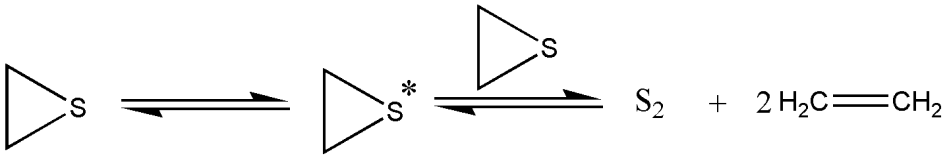

Scheme 1.30 Thermal decomposition of a thiirane to form elemental sulfur and ethylene.

S-S bond oxidation proceeds via oxygen-sulfur coordination, subsequent S-S and/or C-S bond cleavage and/or further oxidation to form a variety of sulfones, sulfoxides and sulfur oxy-acids (scheme 1.31).[65, 71, 136, 137] These species may subsequently decompose yielding products including volatile sulfur oxides (SO_x), unsaturated and saturated hydrocarbons, sulfur compounds and non-volatile high molecular weight species.[65, 123, 125, 138, 139]

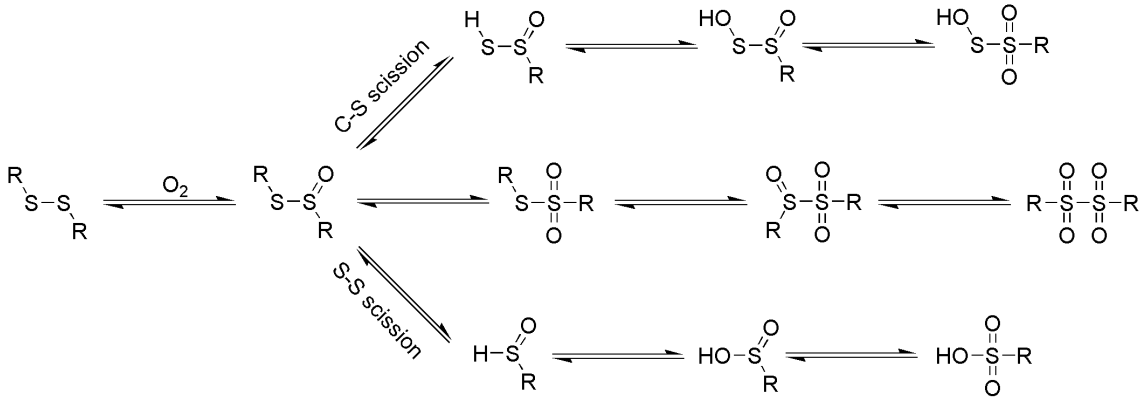

Scheme 1.31 Schematic representation of sulfide oxidation pathways.

Reaction may also occur with C=C bond oxidation products via hydrogen/electron donation (radical scavenging) and/or catalytic decomposition to hinder the generation of

free radicals, giving rise to the anti-oxidant activity of organo-sulfur compounds, which has been studied in great detail.[65, 71, 136, 139] In their investigation into the effects of n-hexyl disulfide and thiophenol on the thermo-oxidative decomposition of dodecane, Morris and Mushrush[71] measured oxygen consumption and hydroperoxide build-up over a series of temperatures for several different additive concentrations. Dodecane oxidation was suppressed by ~ 68 % via the addition of n-hexyl disulfide at 0.2 % sulfur concentration. Thiophenol was found to be considerably more reactive and completely suppressed the formation of hydroperoxides when added at 0.03 % sulfur concentration. The differing activities of the two sulfur compounds were considered according to the mechanisms via which they inhibit the oxidation process. The detection of phenyl disulfide via GCMS analysis of decomposed thiophenol/dodecane provided evidence of thiylphenyl radical formation and dimerisation. The temperatures at which phenyl disulfide was detected were too low for thiylphenyl radicals to be formed as a result of thiophenol thermal decomposition, therefore it was proposed that the thiophenol donated hydrogen via a redox reaction (radical scavenging) with dodecoxy radicals formed by dodecane oxidation. This reaction pathway was considered to be highly favourable due to thiylphenyl radical resonance stabilisation. In contrast, disulfides cannot act as peroxide reducers by donating hydrogen to alkoxy radicals. Although it was considered that disulfide oxidation products such as sulfonic acid may react with dodecoxy radicals to inhibit hydroperoxide formation, no conclusive evidence was found.

Several groups have used thermal analysis techniques including PDSC, TGA and DTA and/or the traditional oxidation techniques outlined in section 1.2.2.2 above to evaluate the anti-oxidant activity of sulfur-containing compounds.[66, 69, 136, 140] Bala et al.[69] used the GFC oxidation test together with viscosity, TAN and insolubles analysis to study the influence of sulfide chemical structure (aromatic vs. aliphatic, mono- vs. di- vs. tri-sulfide) on base oil oxidative stability. The viscosity of the oil generally increased (due to the build up of high molecular weight oxidation products) with increasing sulfur chain length and through the use of cyclic as opposed to aliphatic substitution, whilst steric hinderance was attributed to the lesser viscosity increase observed for *t*-butyl as opposed to *n*-butyl substituted sulfides. Similar observations were made with respect to TAN and

the % insolubles and the following order of the sulfides, from highest to lowest anti-oxidant activity, was obtained: primary/tertiary alkyl monosulfides > primary/tertiary alkyl disulfides > cyclic disulfides/alkyl trisulfides.

The effect of sulfur compound chemical structure (aliphatic sulfide, aromatic sulfide, mercaptan or thiophene) and concentration on the oxidative stability of a lubricating oil was also assessed by Ahmad et al.[136] using DTA and TGA in conjunction with the IP-48 oil oxidation test. Benzo-thiophenes and aliphatic mercaptans were found to be inactive due to their slow reaction with hydroperoxides. However, sulfides were found to successfully inhibit oil oxidation, with aliphatic sulfides exhibiting greater activity than aromatics. In accordance with the observations of Colclough[65] and Willermet et al.[139], Ahmad et al. noted that oxygenated derivatives (such as sulfoxides and thiosulfinates) as opposed to the sulfur compounds themselves functioned as oxidation inhibitors.

Du et al.[140] used RBOT to measure the oxidative stability of mineral oil blended with zinc dialkyl dithiophosphate (ZDTP), ZDTC or ZDTP/ZDTC mixtures and subsequently analysed the oxidised samples using FTIR and PDSC. ZDTP/ZDTC mixtures improved the oil oxidation performance to a greater extent than either of the individual additives. FTIR analysis confirmed the consumption of the anti-oxidants, however some build-up of oil oxidation products was detected. Interestingly, addition of the additives at different concentrations influenced both the shape of the PDSC oil oxidation exotherm as well as the oxidation onset and peak maximum temperatures. In accordance with the RBOT results, the ZDTP/ZDTC mixture increased the main oxidation exotherm peak maximum to higher temperature, indicating improved oxidative stability. However, the onset temperature was lower and this was attributed to the presence of greater levels of primary oxidation products (as opposed to secondary, aged oxidation products) in the ZDTP/ZDTC mixture sample due to inhibition of the oxidation process. Accordingly a small, low-temperature exothermic shoulder on the main oxidation exotherm, attributed to the primary oxidation products, was present in PDSC thermograms of blends exhibiting enhanced anti-oxidant performance. In samples displaying poorer oxidative stability, the low-temperature exotherm was absent and the main exothermic peak was sharper in profile, indicating rapid oil oxidation.

PDSC was also used by Qiu et al.[66] to evaluate the anti-oxidant activities of different organic sulfides in mineral oil and the results were correlated to data obtained by RBOT. OIT was found to be an unsuitable parameter for ranking the anti-oxidant activities of the sulfides due to the significantly different isothermal conditions required to achieve oxidation. Therefore, constant heating-rate analysis was performed and several parameters, including the onset temperature, peak maximum temperature, peak enthalpy and maximum heat flow, were used to rank the stabilities of the oil/sulfide blends towards oxidation. No single parameter accorded to the sequence of the blends determined by RBOT. However, the values were then normalised and summed to give a 'comprehensive index' value, which was found to accurately predict the anti-oxidant activities of the sulfides.

1.2.3.3 Phosphorus-Based Lubrication Additives

The reactions of phosphate-containing lubrication additives with metal surfaces to form thermally-stable decomposition deposits are well-known and form the basis of the AW properties of these compounds.[141] Many authors have investigated the mechanisms via which phosphate additives decompose to form AW films together with how the composition of these films affects lubrication performance.[130, 132, 139, 141-148] However, the majority of studies have focused on two of the most widely used additives, ZDTP[139-142, 149] and tricresyl phosphate (TCP).[143-145, 150]

The preparation of tribochemical films from blends of ZDTP in engine oil base stocks and analysis of the films using reflection-absorption infrared spectroscopy was reported by Willermet et al.[142] The obtained spectra were compared to those of model phosphate glasses and ZDTP thermal and thermo-oxidative degradation products formed in the absence of wear conditions. The results revealed that the tribochemical film spectra were analogous to those obtained for thermo-oxidatively decomposed ZDTP but differed slightly from the phosphate glass model compounds. It was therefore concluded that tribochemical film formation occurred via thermo-oxidative decomposition of the ZDTP to yield a mixture of amorphous short chain $(\text{-O-P-})_n$ compounds (scheme 1.32) such as

orthophosphates and pyrophosphates coordinated to metal cations. Polymeric metaphosphate glasses were not detected.

Willermet et al.[139] subsequently investigated the mechanism of ZDTP film formation in more detail and determined that following ZDTP adsorption and reaction with the metal surface, phosphate film precursors such as thionic acids $(RO)_2P(S)OH$ and phosphorothioate esters $(RO)_2P(S)OR$ were formed by the anti-oxidant activity of the ZDTP sulfur group. It was proposed that the ester groups present in these compounds were then subject to hydrolysis and condensation reactions leading to the growth of a phosphate chain which was terminated by further reaction with metal-containing species. The anti-oxidant activity of ZDTP has also been noted by Du et al.[140] through the performance of RBOT and PDSC analysis (described in section 1.2.3.2 above) and by Sarpal et al.[149] in their study on synergistic additive interactions.

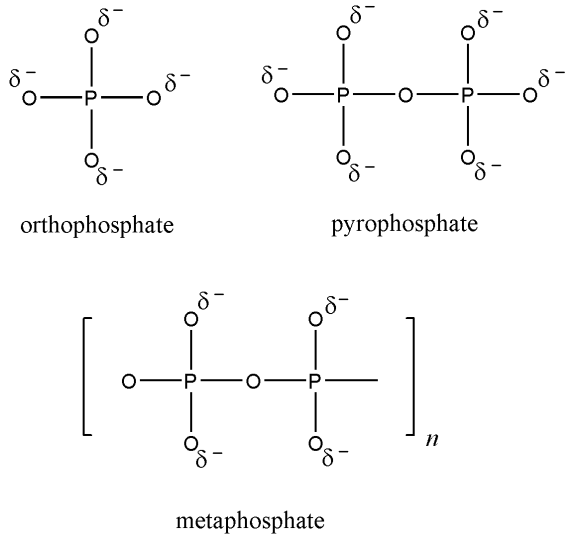

Scheme 1.32 Structural representations of orthophosphate, pyrophosphate and metaphosphate anions.[142]

ZDTP has also been implicated in the formation of engine piston deposits; Smith et al.[133] used various spectroscopic methods to determine that deposit formation commenced via the adsorption of the ZDTP phosphate groups to the metal surface followed by

subsequent thermal and/or oxidative decomposition of the additive to form a variety of phosphates and polyphosphates.

The detection of surface-bound phosphate moieties in the presence and absence of wear conditions has been confirmed by X-ray spectroscopic techniques.[130, 132, 133, 145, 151] Komvopoulos et al.[132] noted that phosphorus-containing AW additives readily reacted with steel surfaces at low (≤ 100 ^{o}C) temperatures and that friction was not required for reaction products to form. Furthermore, phosphorus-containing additives successfully competed with ingredients such as sulfur EP additives and a metal deactivator for sites at the metal surface. These findings were supported by the work of Najman et al., who used XANES to investigate the effect of different phosphorus-containing additives (diphenyl phosphate, triphenyl phosphate and a commercial amine phosphate, Irgalube 349) on tribochemical film thickness and chemical composition[151] and, in a later study, the characteristics of tribo-films formed under both EP and AW conditions by mineral oil blends of the above phosphorus additives with various sulfur-containing EP additives.[130] In both studies, the tribo-films were found to comprise predominantly of iron(II) polyphosphates. Under AW conditions all three phosphate additives competed successfully with the sulfur additives for sites at the steel surface and under EP conditions, diphenyl phosphate and Irgalube were found to preferentially adsorb, blocking adhesion of the sulfur additives.

TCP has been shown to form similar phosphate and polyphosphate-type films to those described for ZDTP. Perez et al.[143] used micro-FTIR to characterise the chemical composition of TCP deposits produced by lubrication and DSC testing. They reported the formation of iron phosphate polymeric species which persisted at temperatures above 600 ^{o}C. Similarly, Arezzo[144] described the aging mechanisms of TCP blends in polar and non-polar functional group-containing hydrocarbon oils on steel at low (~ 100 ^{o}C) temperatures. Whilst surface-bound phosphorus compounds were not detected in the polar oil/TCP blend, polyorganic phosphates were present for the non-polar oil/TCP. However, the amount of phosphate formed for the non-polar oil blend was found to decrease with increasing levels of oil oxidation. These observations were attributed to competition between the TCP phosphate group and polar/oxidised moieties present in

the base oil for adsorption sites at the steel surface.

Several groups have studied the films formed by wear and thermal decomposition of other phosphate-based lubrication additives, however the focus has once again been on lubrication performance.[141] Murase and Ohmori[42] used ToF-SIMS and IRRAS to show that the tribochemical films formed by chemisorption of various triaryl and trialkyl phosphate/phosphite additives on steel sheet comprised of organic iron polyphosphates. Infrared analysis was also used by Komatsuzaki et al.[148] to examine the composition of films formed by reaction between organic acid phosphates and steel during the forward extrusion process. The films formed were comprised of organic iron phosphates and/or pyrophosphates and were effective in preventing welding between the steel and the extrusion workpiece. In a later study, Komatsuzaki and Uematsu[147] assessed the antiseizure performance of a range of phosphorus-based additives in different base oils. The additives, in particular a polyoxyethylene alkylether phosphate diester, increased the maximum workable die temperature by preventing seizure and reducing the load required for forming. This was once again attributed to the formation of phosphorus-containing reaction products at the metal surface.

The research reported by Adhvaryu et al.[146] also described how the tribofilm formed by reaction between an amine phosphonate/chemically-modified vegetable oil blend and steel comprised of a polyphosphate glassy material. However, it was noted that reactions between vegetable oil decomposition products and the phosphorus moiety in the additive to form fatty phosphates resulted in a synergistic effect on lubrication performance.

An extensive investigation into the oxidative degradation of several phosphate esters has been reported by Cho and Klaus,[150] who combined a thin film microoxidation test with Gel Permeation Chromatography (GPC) to study the mechanism and reaction products formed. The phosphate ester oxidation process was shown to be analogous to that of triglycerides, commencing via hydrocarbon chain oxidation followed by the successive formation of low-molecular weight products and high-molecular weight polymerised material. The polymerisation rate constant was roughly four times the primary oxidation rate constant, accounting for the tendency of phosphate esters to form sludge and varnish-like deposits.

Considerably fewer studies have been undertaken to investigate the effects of high – temperature thermal processing on the surface and decomposition reactions of phosphate-based lubrication additives.[152] Mathieu et al.[153] investigated the chemical composition of reaction products formed by the thermal decomposition of several sulfur-containing phosphate esters in a polyalphaolefin base stock by XPS and AES. They found that the additives decomposed temperatures above 400 ^{o}C to form FeS_x and $FePO_4$ reaction layers several nanometres in thickness on the surface of metallic iron. The different additives displayed reactivities which were dependent upon their chemical structure, with a triaryl phosphate ester reacting at temperatures above 700 ^{o}C. It was noted that the absence of mechanical removal of surface layers by wear resulted in a different elemental surface composition due to the presence of greater amounts of oxide.
Substantial research into the thermal and thermo-oxidative decomposition characteristics of various synthetic and commercial phosphate esters using DSC and TGA techniques has been performed by Shankwalkar et al.[154-156] Their findings revealed that phosphate ester chemical structure plays a crucial role in additive thermal stability, with triaryl phosphate esters displaying superior stability towards degradation in comparison to trialkyl and alkyl-aryl derivatives under both oxidising and non-oxidising conditions. Under a nitrogen atmosphere, the DSC thermal degradation onset temperatures measured for triaryl phosphate esters were above 311 ^{o}C, whilst trialkyl and alkyl-aryl phosphate esters showed degradation at temperatures below 285 ^{o}C.[154] The oxidation onset temperatures measured for the phosphate esters were much lower, ranging from ≥ 200 ^{o}C for triaryl phosphates down to 150-200 ^{o}C for trialkyl and alkyl-aryl phosphates.[155] These observations were ascribed to differences in the resistance of the hydrocarbon portion of the additives to thermal and oxidative degradation; aromatic groups possess enhanced thermal stability in comparison to aliphatic derivatives and are more resistant to hydrogen abstraction (oxidation initiation). Interestingly, whilst a relationship between additive molecular weight and TGA mass loss was established under an oxygen atmosphere, no such relationship was observed under nitrogen. This was associated with a lack of instrumental sensitivity, however it is not obvious why a difference in ‘sensitivity’ was observed under the two different gas atmospheres.

Shankwalkar et al. then compared the DSC and TGA results to determine whether additive mass loss was due to thermal degradation, oxidation or evaporation. Under nitrogen it was found that the initial mass loss undergone by all three types of phosphate ester resulted from evaporation as opposed to the evolution of thermal degradation products; volatilisation occurred at lower temperatures than the onset temperature of thermal degradation by DSC. In contrast, for many of the additives studied under an oxygen atmosphere, the TGA onset temperature of mass loss was greater than the oxidation onset by DSC such that mass loss was due to oxidative as well as evaporative phenomena. Only *tert*-butylphenyl phosphate esters underwent evaporation prior to the commencement of oxidative decomposition reactions. Despite the extensive nature of this research, Shankwalkar et al. did not investigate the reactions giving rise to phosphate ester mass loss during the more advanced stages of the thermal and thermo-oxidative decomposition processes; the additives were only studied up to the 10 % mass loss level. Furthermore, no findings made concerning the relationship between phosphate ester chemical structure and the composition of residues present at temperatures above 350 ^{o}C.

Residue levels formed by thermal decomposition of phosphate materials have been assessed more extensively in relation to fire retardant additives[157, 158] and materials.[159] Kettrup et al.[158] used thermal analysis techniques coupled with mass spectrometry to characterise the thermal decomposition of various phosphate-based fire retardant additives in air and under an inert atmosphere. The majority of additives decomposed via a two-stage mass loss process by TGA and formed significant amounts of ‘char-like’ residue which persisted to temperatures up to 700 ^{o}C.

In summary, the thermal and thermo-oxidative decomposition processes undergone by a variety of different phosphate-based AW additives in the presence and absence of wear conditions have been studied extensively by a range of thermal analysis and spectroscopic methods. Although surface reactivity, high thermal and oxidative stability and low volatility have been identified as critical to the performance of phosphate-based additives in both lubrication and fire retardant applications, where metal surface cleanliness is crucial to the integrity of further treatments the persistence of phosphate

additive decomposition deposits may be detrimental. No studies have been undertaken to investigate the impact of phosphate lubrication additive-derived residues on hot dip metallic coating quality.

1.3 Research Aims and Scope

A review of the literature reveals that although rolling oil-derived residues are frequently cited as being detrimental to hot dip metallic coating quality and giving rise to the formation of uncoated defects, the majority of studies into the effect of processing conditions on hot dip metallic coating quality have focused on substrate oxidation and preheat temperature. No investigations have been specifically directed towards investigating the relationships between oil-derived residues and uncoated defect formation. Furthermore, little is known concerning the chemical nature of oil-derived steel surface residues, the processes via which such residues are formed during steel furnace cleaning and the effects of rolling oil formulation composition on residue formation (i.e. whether/which specific rolling oil ingredients are primarily responsible for giving rise to the formation of high residue levels).

In contrast, considerable knowledge exists regarding the process of automotive lubricant thermo-oxidative decomposition and a range of analytical techniques have been employed to study this process. Of these techniques, TGA and PDSC offer the greatest advantages including short experimental timeframe, small sample size, ease of sample preparation and flexibility in tailoring test conditions. However, the majority of studies have investigated the comparative stabilities of different lubricants towards oxidation and/or the kinetics of the thermo-oxidative decomposition process. Less is known about lubricant thermo-oxidative decomposition at temperatures above the onset temperature of oxidation. An useful PDSC-based technique for evaluating the deposit-forming tendencies of engine oils was developed by Zhang et al. in the early 1990’s, however attempts by Quaker Chemical to modify this technique for the evaluation of cold rolling oils have had limited success.

In relation to the residue-forming tendencies and thermo-oxidative decomposition

processes of particular rolling oil components, triglycerides and semi-/fully-synthetic base esters, sulfurised EP additives and phosphorus AW additives have been investigated in great detail with regard to applications in the food and lubricant industries. The tendency of these classes of compounds to form thermally-stable decomposition deposits is well-known and the chemical structure of such deposits has been identified in many cases. However, this information has not been applied in the context of the steel cold rolling/hot dip metallic coating process such that potential links between deposits formed by these compounds and the formation of uncoated defects are unsubstantiated.

Given this context, the primary aim of the present study was to gain a more detailed understanding of how cold rolling oils and their thermal decomposition residues impact upon the formation of uncoated defects in 55Al-43.4Zn-1.6Si hot dip metallic coatings, as shown in figure 1.8.

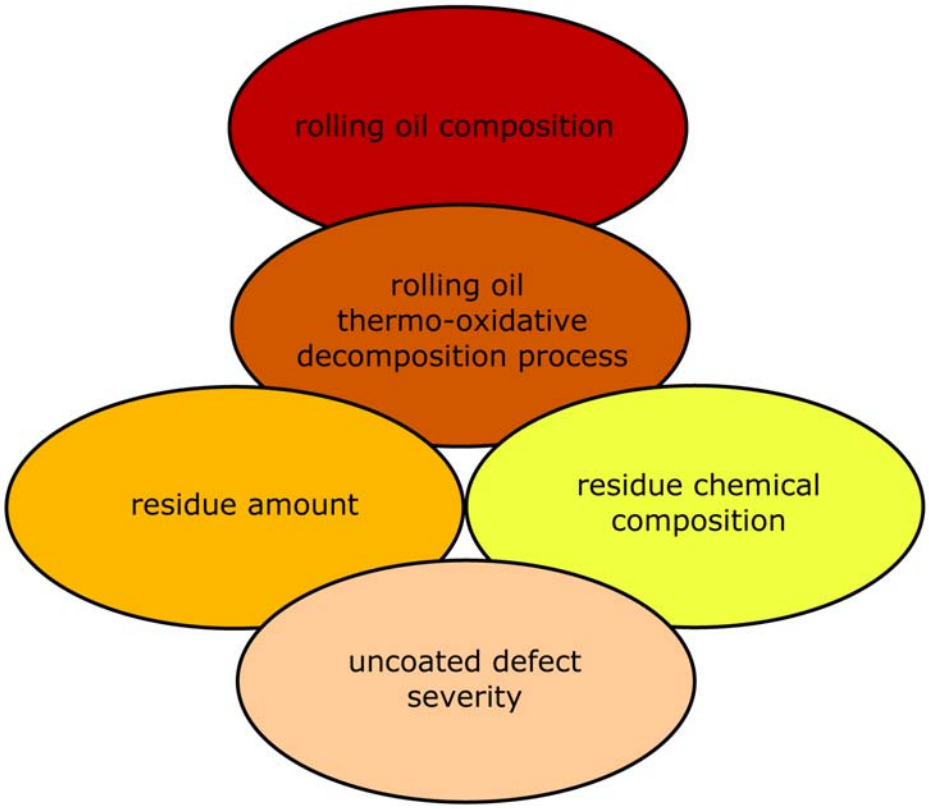

Figure 1.8 Overview of the aim of this thesis.

Knowledge was desired concerning:

- which classes of rolling oil ingredients are primarily associated with the formation of uncoated defects in 55Al-43.4Zn-1.6Si hot dip coatings;
- relationships between uncoated defect severity and the amount/chemical composition of residues formed by rolling oil/ingredient thermal decomposition;
- the processes via which rolling oil ingredients decompose under thermo-oxidising and thermo–reducing conditions to leave thermally-stable residues and the chemical nature of these residues;
- how variations in the chemical structure of rolling oil ingredients within specific ingredient classes influences the amount/process of formation of thermally-stable decomposition residues;
- the effect of different industrial process variables, such as furnace gas composition and the availability/concentration of iron, on the rolling oil thermal decomposition and residue formation processes, and
- methods for screening rolling oils/ingredients with respect to their likely impact upon hot dip metallic coating quality.

Answers to these questions will facilitate the development of improved cold rolling oil formulations and aid in the optimisation of furnace cleaning conditions for enhanced hot dip metallic coating quality.

Given the vast variety of cold rolling oil/steel/hot dip metallic coating compositions and furnace cleaning processes and the numerous different variables that can potentially impact upon residue/uncoated defect formation, the scope of this research was limited considerably. The impact of the cold rolling process and coil storage on rolling oil decomposition has been investigated comprehensively by others and is not considered in the present study. Therefore, the rolling oils used have not been applied as emulsions; neat oils have been used as the majority of water is evaporated during the rolling process, leaving the residual rolling oil film. Similarly, this research primarily involves cold rolling oils/ingredients used in the steel (as opposed to aluminium) cold rolling process.

55Al-43.4Zn-1.6Si alloy is the only hot dip metallic coating alloy investigated; other coating compositions are not considered, nor are other processes for coating deposition. 'Hot dip metallic coating quality' has been determined with reference to uncoated defect severity (evaluated by defect size and surface coverage) as opposed to metallurgical aspects such as intermetallic phase/alloy overlayer composition and microstructure.

A single grade of steel (G550, refer to table 2.3 in Chapter 2 and table 1.1 above) was used as the G550/55Al-43.4Zn-1.6Si combination represents BlueScope's most common alloy coated product. Despite this narrow scope, findings made using this alloy coating/steel grade combination may be applicable to other steels and metallic coatings.

The primary cleaning process considered in this research is the continuous annealing process, whereby the cold rolling oil film is removed within an atmosphere containing natural gas combustion products. Therefore, thermo-oxidative have been employed to simulate the partially-oxidised state of the cold rolling oil when it enters the continuous annealing furnace and the availability of oxygen-containing species at the steel surface (iron oxides) and in the furnace atmosphere (water, carbon monoxide, carbon dioxide and a small amount of molecular oxygen) for reaction with the rolling oil. A reducing HNX atmosphere has also been employed in many sections of this work such that findings may also be relevant to the batch annealing process. Alternative steel cleaning processes such as electrolytic and solvent degreasing are not considered as they are not used extensively within Australia by BlueScope Steel® and they have been studied by others.[49]

1.4 Thesis Outline

Chapter 2 describes the general materials, sample preparation methods and characterisation techniques employed throughout this research; details pertaining to particular aspects of this work are provided in the relevant chapters.

A review of the literature has shown that thermally-stable rolling oil-derived residues remaining on the steel surface following the cold rolling and furnace cleaning processes can cause the formation of bare spot, or uncoated, defects and therefore have a

detrimental effect upon 55Al-43.4Zn-1.6Si alloy coating quality. Identification of key rolling oil ingredients which thermo-oxidatively decompose to form residues which give rise to uncoated defects is of particular interest. *Chapter 3* therefore investigates residue formation in the most prevalent and easily-modified class of rolling oil ingredients: esters. In *3.1*, methyl esters are used as model compounds to evaluate the dependency of the thermo-oxidative decomposition process and its products on ester alkyl chain unsaturation levels. This work is expanded upon in *3.2*, whereby the residue-forming characteristics of a range of triglycerides and semi-/fully-synthetic commercial base esters of varying fatty acid composition are studied by PDSC, TGA and infrared spectroscopic techniques. A variation of Zhang et al.'s PDSC 2-peak technique[25, 83, 84] is used to assess the residue-forming tendencies of the esters and the characteristics of ester residue formation under thermo-oxidative conditions are contrasted to those under a thermo-reductive HNX environment. Industrial and experimental hot dipping trials are performed to evaluate the impact of several of the esters upon 55Al-43.4Zn-1.6Si coating quality. The resultant uncoated defect severity is determined by visual, optical microscopy and SEM analysis and related back to ester chemical structure and residue amount/composition.

Sulfur- and phosphorus-containing lubrication additive were identified in the literature review as promoting the formation of high levels of residue in a variety of lubricants. Given the widespread use these additives in commercial cold rolling oil formulations, *Chapter 4* describes an analogous investigation utilising several different sulfur- and phosphorus-containing lubrication additives in both neat and ester-blended forms to that undertaken in Chapter 3.

In Chapters 3 and 4 an aluminium substrate is employed in all thermal analysis and infrared studies to preclude interference from substrate oxidation and enhance PDSC test reproducibility. In order to rationalise these results within a context more closely aligned to industrial conditions, the effects of substrate composition and furnace atmosphere on the decomposition of a fully-formulated cold rolling oil are explored in *Chapter 5*. In *5.1*, iron is introduced into the rolling oil testing regime in the form of a cold rolled steel substrate and iron oxide powder, which is used to increase the iron-to-oil ratio and

mimic the availability of iron fines formed by wear during cold rolling. The rolling oil thermo-oxidative decomposition process is monitored by TGA under these two conditions and compared to that using an aluminium substrate. Furthermore, high temperature laser scanning confocal microscopy is used to visualise the process of rolling oil removal from the cold rolled steel surface. The impact of four different furnace atmospheres, from non-oxidising through to highly oxidising, on the oil decomposition process in the presence of a steel substrate is then evaluated by TGA in *5.2*. The activation energy associated with oil decomposition events is calculated in both sections by Modulated Thermogravimetry (MTGA) and the Flynn-Wall-Ozawa method.[160-162]

The impact of rolling oil formulations upon metallic coating quality is currently evaluated by performing industrial hot dip coating trials. These trials are both time-consuming and costly so that a rapid, laboratory-based screening method is required to facilitate the formulation of improved rolling oils. The development of such a method, based upon TGA and PDSC analysis techniques, is described in *Chapter 6*.

Finally, the conclusions drawn from this work together with recommendations for future research are summarised in *Chapter 7*.

1.5 References

1. Ferber, P. The Australian Steel Industry in 2003. http://www.industry.gov.au/assets/documents/itrinternet/Steel0320040520152158.pdf (10/07/07).

2. BlueScope Steel 2005/2006 annual report: transforming our business. http://www.bluescopesteel.com/go/investors/annual-reports (06/07/07).

3. BlueScope Steel: ZINCALUME steel G550, G550S datasheet. http://www.bluescopesteel.com.au/go/product/zincalume-g550-g550s-steel# (06/07/07).

4. Hudson, R. M., Pickling and Descaling. In *ASM Handbook - Surface Engineering*; ASM International (The Materials Information Society): 1994; 'Vol.' 5, pp 67.

5. Gibson, A., Pers. Comm. In 2003.

6. Blanco, A., Renshaw, W., *Thermogravimetric set-up for oil volatility tests*; BHP Steel: 1998; pp 1.
7. Blanco, A., Took, P., *The effects of slow coil cooling on the ageing and volatility of cold rolling lubricants - part 2*; BHP Steel: 1999; pp 1.
8. Blanco, A., Took, P., *The effects of slow coil cooling on the ageing and volatility of cold rolling lubricants*; BHP Steel: 1999; pp 1.
9. Shamaiengar, M., *Iron Steel Eng.* **1967,** *44*, 135.
10. Gamlin, C. D., Dutta, N. K., Choudhury, N. R., Kehoe, D., Matisons, J., *Thermochim. Acta* **2002,** *392-393*, 357.
11. Fox, N. J., Stachowiak, G. W., *Lubr. Eng.* **2003,** *59*, 15.
12. Svedung, D. H., *Scand. J. Metall.* **1980,** *9*, 183.
13. Willem, J.-F., Claessens, S., Cornil, H., Fiorucci, M., Hennion, A., Xhoffer, C. In *Solidification mechanisms of aluzinc coatings - effect on spangle size*, Galvatech '01 - Proc. 5th Int. Conf. on Zinc and Zinc Alloy Coated Steel Sheet, Brussels, Belgium; 2001, pp 401.
14. Chen, R. Y., Willis, D. J., *Metall. Mater. Trans. A* **2005,** *36A*, 117.
15. Browne, K. M. Available energy: unified concepts for classical and irreversible thermodynamics. Deakin University, Geelong, 2001.
16. Servais, J. P., Leroy, V., Application of surface analysis in steel industry. In *Secondary Ion Mass Spectrometry*, Huber, A., Benninghoven, A., Werner, H., 'Ed."; Wiley: Chichester, 1988; pp 551.
17. Renshaw, W., Pers. Comm. In 2003.
18. Evans, C. An anecdotal history of the galvanizing industry. http://www.galvanizeit.org/resources/files/AGA%20PDFs/ms_hist_92.pdf (10/07/07).
19. Atkins, P. W., *Physical Chemistry, 6th edition*. Oxford University Press: New York, 1999.
20. Townsend, H. E., Continuous Hot Dip Coatings. In *ASM Handbook - Surface Engineering*; ASM International (The Materials Information Society): 1994; 'Vol.' 5, pp 339.
21. Tang, N.-Y., Goodwin, F. E. In *A study of defects in galvanized coatings*, Galvatech

'01 - Proc. 5th Int. Conf. on Zinc and Zinc Alloy Coated Steel Sheet, Brussels, Belgium; 2001, pp 49.
22. Chen, F., Patil, R. In *An in-depth analysis of various subtle coating defects of the 2000's*, Galvatech '04 - Proc. 6th Int. Conf. on Zinc and Zinc Alloy Coated Steel Sheet, Chicago, USA; 2004, pp 1055.
23. Williams, J., Dippenaar, R., Phelan, D., Renshaw, W. In *Condensation of zinc vapour on steel strip in a reducing atmosphere*, Galvatech '04 - Proc. 6th Int. Conf. on Zinc and Zinc Alloy Coated Steel Sheet, Chicago, USA; 2004, pp 951.
24. Browne, K. M., *Zincalume pinhole uncoated investigation: progress report*; 726; John Lysaght (Australia) Limited: April, 1980; pp 1.
25. Evans, R., Frelin, J., Morrison, S., *Measurement of the oxidative polymerisation properties of rolling oil lubricants using the PDSC technique, and its relationship to Zincalume coating compatibility at BHP Steel Port Kembla*; Quaker Chemical Corporation Corporate Technology Laboratory: 6th November, 1998; pp 1.
26. Puente, J. M., Alonso, F. J., Andres, L., Prado, M. In *Influence of an adequate surface conditioning on the final characteristics of GI for exposed panels use on automotive sector*, Galvatech '04 - Proc. 6th Int. Conf. on Zinc and Zinc Alloy Coated Steel Sheet, Chicago, USA; 2004, pp 457.
27. Dionne, S., Voyzelle, B., Li, J., Essadiqi, E., Baril, E., McDermid, J. R., Goodwin, F. In *Effect of reheating parameters of galvanizing behaviour and properties of high strength hot rolled steels*, Galvatech '04 - Proc. 6th Int. Conf. on Zinc and Zinc Alloy Coated Steel Sheet, Chicago, USA; 2004, pp 751.
28. Maeda, S., *Adhes. Aspects of Polym. Coat.* **2003,** *2*, 165.
29. Durandet, Y., Strezov, L., Ebrill, N. In *Formation of Al-Zn-Si coatings on low carbon steel substrates*, Galvatech '98 - Proc. 4th Int. Conf. on Zinc and Zinc Alloy Coated Steel Sheet, Chiba, Japan; 1998, pp 147.
30. Durandet, Y., Ebrill, N., Strezov, L. In *Influence of substrate oxidation on dynamic wetting, interfacial resistance and surface appearance of Al-Zn-Si hot dip coatings*, Proc. PacZAC '99, Kuala Lumpur, Malaysia; 1999.
31. Ebrill, N., Durandet, Y., Strezov, L. In *Influence of substrate oxidation on dynamic*

wetting, interfacial resistance and surface appearance of hot dip coatings, Galvatech '01 - Proc. 5th Int. Conf. on Zinc and Zinc Alloy Coated Steel Sheet, Brussels, Belgium; 2001, pp 351.

32. Ebrill, N., Durandet, Y., Strezov, L., *Metall. Mater. Trans. B* **2000,** *31B*, 1069.

33. Ebrill, N., Durandet, Y., Strezov, L., *Trans JWRI* **2001,** *30*, 351.

34. Ebrill, N., Durandet, Y., Strezov, L. In *Dynamic reactive wetting and its role in hot dip coating*, ISS Belton Symposium, Sydney, Australia; 2000, pp 303.

35. Keyser, A. G., Kunkel, K. F., Snedaker, L. A., *Iron Steel Eng.* **1998,** *75*, 43.

36. Sech, J. M., Oleksiak, T. P., *Iron Steel Eng.* **1995,** *72*, 33.

37. Fujioka, Y., Tanikawa, K. In *An approach to the clarification of the lubricating performance of cold rolling oils by a new analytical method*, Proc. 41st Chem. Conf., 1988, pp 83.

38. Tusset, V., Muller, V., *Chemical analysis of oils present on steel sheet*; EUR 14113; 1992; pp 108.

39. Hombek, R., Heenan, D. F., Januszkiewicz, K. R., Sulek, H. H., *Lubr. Eng.* **1989,** *45*, 56.

40. Tanikawa, K., Fujioka, Y., *Lubr. Eng.* **1984,** *40*, 715.

41. De Werbier, P., Hocquaux, H., Flandin-Rey, Y., Jacquet, D., *Development of new methods of analysis for organic compounds on the surface of steel products*; EUR 14113; Luxembourg, 14-16 May 1991, 1992; pp 101.

42. Murase, A., Ohmori, T., *Surf. Interface Anal.* **2001,** *31*, 93.

43. Tamai, Y., Sumimoto, M., *Lubr. Eng.* **1975,** *31*, 81.

44. Hanaki, K., *Sumimoto Light M. Tech.* **1984,** *25*, 44.

45. Pilon, A. C., Cole, K. C., Noel, D. In *Surface characterization of cold-rolled steel by grazing-angle reflection-absorption FT-IR spectroscopy*, SPIE Proc. - 7th Int. Conf. on Fourier Transform Spectrosc., 1989, pp 209.

46. Cole, K. C., Pilon, A., Noel, D. In *FT-IR analysis of oil emulsions used in the cold rolling of steel*, SPIE Proc. - 7th Int. Conf. on Fourier Transform Spectrosc., 1989, pp 123.

47. Chopra, A., Sastry, M. I. S., Kapur, G. S., Sarpal, A. S., Jain, S. K., Srivastava, S. P.,

Bhatnagar, A. K., *Lubr. Eng.* **1995,** *52*, 279.

48. Payling, R., Coated Steel. In *Surface Analysis Methods in Materials Science*, O'Connor, D. J., Sexton, B. A., Smart, R. St. C., 'Ed."; Springer-Verlag: New York, USA, 1992; 'Vol.' 23, pp 387.

49. Shaw, G. S. The effect of processing variables on steel surface chemistry. PhD Thesis, Case Western Reserve University, Cleveland, 1993.

50. Treverton, J. A., Thomas, M. P., *Int. J. Adhes. Adhes.* **1989,** *9*, 211.

51. Mercer, P. D., Payling, R., *Nuclear Instrum. Meth.* **1981,** *191*, 283.

52. Johannessen, J. S., Grande, A. P., Notevarp, T., *Mater. Sci. Eng.* **1980,** *42*, 321.

53. Hunault, P., Maul, C. Glow discharge - a modern concept for coatings analysis. http://www.leco.com/resources/articles_&_references_subs/pdf/milsteel.pdf (10/07/07).

54. Dauchot, G., Combarieu, R., Montmitonnet, P., Repoux, M., Dessacles, G., Delamare, F., *Rev. Metall. / Cah. Inf. Tech.* **2001,** *98*, 159.

55. Toujou, F., Tsukamoto, K., Matsuoka, K., *Appl. Surf. Sci.* **2003,** *203-204*, 590.

56. Reich, R. A., Epp, J. M., Festa, R. P., *Lubr. Eng.* **1994,** *50*, 31.

57. Bexell, U., Carlsson, P., Olsson, M., *Appl. Surf. Sci.* **2003,** *203-204*, 596.

58. Bexell, U., Olsson, M., *Surf. Interface Anal.* **2001,** *31*, 212.

59. deVries, J. E., *J. Mater. Eng. Perf.* **1998,** *7*, 303.

60. Lafargue, P. E., Chaoui, N., Millon, E., Muller, J. F., Derule, H., Popandec, A., *Surf. Coat. Technol.* **1998,** *106*, 268.

61. Gines, M. L. J., Benitez, G. J.,Perez, T., Bossi, E. In *Surface reactions during batch annealing process*, Proc. 55th Annual ABM Congress, Rio de Janeiro; 2000, pp 2239.

62. Suilen, F., Zuurbier, S. In *Fundamental aspects of gas-metal reactions during batch annealing in 100% hydrogen*, Proc. 38th Mechanical Working and Steel Processing Conference, Ohio, USA; 1997, pp 375.

63. Osten-Sacken, J., Pompe, R., Skold, R., *Thermochim. Acta* **1985,** *95*, 431.

64. Bowman, W. F., Stachowiak, G. W., *Lubr. Eng.* **1998,** *54*, 19.

65. Colclough, T., *Ind. Eng. Chem. Res.* **1987,** *26*, 1888.

66. Qiu, C., Han, S., Cheng, X., Ren, T., *Thermochim. Acta* **2006,** *447*, 36.

67. Jain, M. R., Sawant, R., Paulmer, R. D. A., Ganguli, D., Vasudev, G., *Thermochim.*

Acta **2005,** *435*, 172.
68. Adhvaryu, A., Erhan, S. Z., Sahoo, S. K., Singh, I. D., *Fuel* **2002,** *81*, 785.
69. Bala, V., Hartley, R. J., Hughes, L. J., *Lubr. Eng.* **1996,** *52*, 868.
70. Ripley, D. L., Chirico, R. D., Steele, W. V., Kamin, R. A. In *Differential scanning calorimetry: a new technique for fuel thermal oxidative stability studies*, Proc. 4th Int. Conf. on Stability and Handling of Liquid Fuels, Orlando, Florida, USA; 1991, pp 301.
71. Morris, R. E., Mushrush, G. W., *Prepr. Pap. - Am. Chem. Soc., Div. Fuel Chem.* **1989,** *34*, 538.
72. Abou El Naga, H. H., Salem, A. E. M., *Wear* **1984,** *96*, 267.
73. Rhee, I.-S., *NLGI Spokesman* **2001,** *65*, 16.
74. Sisk, B., Zou, D., Pan, W., Riga, A. In *Effects of brand, grade, and fuel contamination upoin the thermal stability of motor oils*, Proc. 27th Conference of the North American Thermal Analysis Society, Savannah, Georgia; 1999, pp 414.
75. Santos, J. C. O., Santos, I. M. G., Souza, A. G., Sobrinho, E. V., Fernandes Jr., V. J., Silva, A. J. N., *Fuel* **2004,** *83*, 2393.
76. Rhee, I.-S. In *Development of a new oxidation stability test method for greases using a pressure differential scanning calorimeter*, NLGI 27th Annual Meeting, Denver, USA; 1990, pp 1.
77. Senthivel, P., Joseph, M., Nagar, S. C., Anoop, K., Naithani, K. P., Mehta, A. K., Raje, N. R., *NLGI Spokesman* **2005,** *69*, 26.
78. Zeman, A., Stuwe, R., Koch, K., *Thermochim. Acta* **1984,** *80*, 1.
79. Kauffman, R. E., Rhine, W. E., *Lubr. Eng.* **1988,** *44*, 154.
80. Adamczewska, J. Z., Love, C., *J. Therm. Anal. Cal.* **2005,** *80*, 753.
81. Sharma, B. K., Stipanovic, A. J., *Thermochim. Acta* **2003,** *402*, 1.
82. Bowman, W. F., Stachowiak, G. W., *Tribol. Int.* **1996,** *29*, 27.
83. Zhang, Y., Pei, P., Perez, J. M., Hsu, S. M., *Lubr. Eng.* **1992,** *48*, 189.
84. Zhang, Y., Perez, J. M., Pei, P., Hsu, S. M., *Lubr. Eng.* **1992,** *48*, 221.
85. Cheenkachorn, K., Lloyd, W. A., Perez, J. M. In *The use of pressurized differential scanning calorimetry (PDSC) to evaluate effectiveness of additives in vegetable oil lubricants*, ASME ICES03, Spring Technical Conference, Internal Combustion Engine

Division, Saltzburg; May 11-15, 2003, pp 197.

86. Biresaw, G., Adhvaryu, A., Erhan, S. Z., Carriere, C. J., *JAOCS* **2002,** *79*, 53.

87. Hasenhuettl, G. L., Fats and Fatty Oils. In *Kirk-Othmer Encyclopedia of Chemical Technology*, Kroschwitz, J. I., 'Ed."; John Wiley & Sons: New York, 2005; pp 801.

88. Varma, R. P., Shukla, S. S., *Tenside Det.* **1983,** *20*, 192.

89. Upadhyaya, S. K., Sharma, P. S., *Asian J. Chem.* **1997,** *9*, 388.

90. Lanjewar, R. B., Garg, A. N., *Indian J Chem.* **1991,** *30A*, 350.

91. Mehrotra, K. N., Saroha, S. P. S., Kachhwaha, R., *Tenside Det.* **1981,** *18*, 28.

92. Singh, C., Upadhyaya, S. K., *Asian J. Chem.* **2001,** *13*, 977.

93. Yeganeh, H., Mehdizadeh, M. R., *Eur. Polym. J.* **2004,** *40*, 1233.

94. Yeganeh, H., Shamekhi, M. A., *J. Appl. Polym. Sci.* **2005,** *99*, 1222.

95. Dias, F. M., Lahr, F. A. R., *Mater. Res.* **2004,** *7*, 413.

96. Frankel, E. N., *Prog. Lipid Res.* **1985,** *23*, 197.

97. Porter, N. A., Mills, K. A., Carter, R. L., *J. Am. Chem. Soc.* **1994,** *116*, 6690.

98. Coni, E., Podesta, E., Catone, T., *Thermochim. Acta* **2004,** *418*, 11.

99. Oyman, Z. O. Towards environmentally friendly catalysts for alkyd coatings. Eindhoven University of Technology, Eindhoven, 2005.

100. Oyman, Z. O., Ming, W., van der Linde, R., *Prog. Org. Coat.* **2005,** *54*, 198.

101. Adhvaryu, A., Erhan, S. Z., Liu, Z. S., Perez, J. M., *Thermochim. Acta* **2000,** *364*, 87.

102. Christensen, P. A., Egerton, T. A., Lawson, E. J., Temperley, J., *J. Mater. Sci.* **2002,** *37*, 3667.

103. Chang, J. C. S., Guo, Z., *Atmosph. Environ.* **1998,** *32*, 3581.

104. Russell, G. A., *J. Am. Chem. Soc.* **1957,** *79*, 3871.

105. Russell, G. A., *J. Am. Chem. Soc.* **1956,** *78*, 1047.

106. Hancock, R. A., Leeves, N. J., *Prog. Org. Coat.* **1989,** *17*, 321.

107. Aoudin-Jirackova, L., Verdu, J., *J. Polym. Sci., Part A: Polym. Chem.* **1987,** *25*, 1205.

108. Rice, F. O., Herzfeld, K. F., *J. Am. Chem. Soc.* **1934,** *56*, 284.

109. Ninan, K. N., Krishnan, K., Rao, K. V. C. In *A thermogravimetric study of the*

catalytic decomposition of non-edible vegetable oils, Thermal Analysis - Proc. 7th Int. Conf. on Thermal Analysis, 1982, pp 1197.

110. Kodali, D. R., *J. Agric. Food Chem.* **2005,** *53*, 7649.

111. Kowalski, B., Ratusz, K., Kowalska, D., Bekas, W., *Eur. J. Lipid Sci. Technol.* **2004,** *106*, 165.

112. Kowalski, B., Gruczynska, E., Maciaszek, K., *Eur. J. Lipid Sci. Technol.* **2000,** *102*, 337.

113. Kowalski, B., *Thermochim. Acta* **1993,** *213*, 135.

114. Tan, C. P., Che Man, Y. B., *Food Chem.* **1999,** *67*, 177.

115. Kasprzycka-Guttman, T., Odzeniak, D., *J. Therm. Anal.* **1993,** *39*, 217.

116. Dweck, J., Sampaio, C. M. S., *J. Therm. Anal. Cal.* **2004,** *75*, 385.

117. Santos, J. C. O., Santos, I. M. G., Conceicao, M. M., Porto, S. L., Trindade, M. F. S., Souza, A. G., Prasad, S., Fernandes, V. J., Araujo, A. S., *J. Therm. Anal. Cal.* **2004,** *75*, 419.

118. Shen, L., Alexander, K. S., *Thermochim. Acta* **1999,** *340-341*, 271.

119. Sathivel, S., Prinyawiwatkul, W., Negulescu, I., King, J., Basnayake, B., *J. Am. Oil Chem. Soc.* **2003,** *80*, 1131.

120. Dunn, R., *Trans. ASABE* **2006,** *49*, 1633.

121. Akiba, M., Hashim, A. S., *Prog. Polym. Sci.* **1997,** *22*, 475.

122. Benassi, R., Taddei, F., *J. Comput. Chem.* **2000,** *21*, 1405.

123. Martin, G., Pyrolysis of organosulfur compounds. In *The chemistry of sulfur-containing functional groups*, Patai, S., 'Ed."; John Wiley and Sons Ltd: 1993; pp 395.

124. Herrendorf, L., Sulfur donors-part II. In; Quaker Chemical: 2005; pp 1.

125. Voronkov, M. G., Deryagina, E. N., Thermal reactions and high temperature syntheses of organosulfur compounds. In *Chemistry of Organosulfur Compounds: General Problems*, Belen'kii, L. I., 'Ed."; Ellis Horwood: New York, 1990; pp 48.

126. Fabuss, B. M., Duncan, D. A., Smith, J. O., Satterfield, C. N., *Ind. Eng. Chem. Proc. Des. Dev.* **1965,** *4*, 117.

127. Gonzalez, L., Rodriguez, A., Del Campo, A., Marcos-Fernandez, A., *J. Appl. Polym. Sci.* **2002,** *85*, 491.

128. Lara, J., Blunt, T., Kotvis, P., Riga, A., Tysoe, W. T., *J. Phys. Chem. B* **1998,** *102*, 1703.

129. Kim, S. M., Sit, C. Y., Komvopoulos, K., Yamaguchi, E. S., Ryason, P. R., *Tribol. Trans.* **2000,** *43*, 569.

130. Najman, M. N., Kasrai, M., Bancroft, G. M., *Wear* **2004,** *257*, 32.

131. Najman, M. N., Kasrai, M., Bancroft, G. M., *Tribol. Lett.* **2003,** *14*, 225.

132. Komvopoulos, K., Do, V., Yamaguchi, E. S., Yeh, S. W., Ryason, P. R., *Tribol. Trans.* **2004,** *47*, 321.

133. Smith, G. C., Hopwood, A. B., Titchener, K. J., *Surf. Interface Anal.* **2002,** *33*, 259.

134. Riga, A. T., Hong, H., Kornbrekke, R. E., Cahoon, J. M., Vinci, J. N., *Lubr. Eng.* **1992,** *49*, 65.

135. Sundarrajan, S., Surianarayanan, M., Srinivasan, K. S. V., *J. Polym. Sci., Part A: Polym. Chem.* **2005,** *43*, 638.

136. Ahmad, L. A., Eissa, E. A., Taman, A. R., *Erd. Koh. Erdg. Petr. V.* **1991,** *44*, 151.

137. Block, E., Ahmad, S., Catalfamo, J. L., Jain, M. K., Apitz-Castro, R., *J. Am. Chem. Soc.* **1986,** *108*, 7045.

138. Penn, R. E., Block, E., Revelle, L. K., *JACS* **1978,** *100*, 3622.

139. Willermet, P. A., Dailey, D. P., Carter III, R. O., Schmitz, P. J., Zhu, W., *Tribol. Int.* **1995,** *28*, 177.

140. Du, D., Kim, S. -S., Moon, W. -S., Jin, S. -B., Kwon, W. -S., *Thermochim. Acta* **2003,** *407*, 17.

141. Han, S.-Y., Yi, J. -J., *ISIJ Int.* **1997,** *37*, 498.

142. Willermet, P. A., Carter III, R. O., Boulos, E. N., *Tribol. Int.* **1992,** *25*, 371.

143. Perez, J. M., Ku, C. S., Pei, P., Hegemann, B. E., Hsu, S. M., *Tribol. Trans.* **1990,** *33*, 131.

144. Arezzo, F., *ASLE Trans.* **1985,** *28*, 203.

145. Ma, Y., Liu, J., Zheng, L., *Tribol. Int.* **1995,** *28*, 329.

146. Adhvaryu, A., Erhan, S. Z., Perez, J. M., *Wear* **2004,** *257*, 359.

147. Komatsuzaki, S., Uematsu, T., *Lubr. Eng.* **1995,** *51*, 653.

148. Komatsuzaki, S., Nakano, F., Uematsu, T., Narahara, T., *Lubr. Eng.* **1985,** *41*, 543.

149. Sarpal, A. S., Christopher, J., Mukherjee, S., Patel, M. B., Kapur, G. S., *Lubr. Sci.* **2005,** *17*, 319.

150. Cho, L., Klaus, E. E., *ASLE Trans.* **1981,** *24*, 119.

151. Najman, M. N., Kasrai, M., Bancroft, G. M., Miller, A., *Tribol. Lett.* **2002,** *13*, 209.

152. Gschwender, L. J., Snyder, C. E., Fultz, G. W., Chen, L. S., *Lubr. Eng.* **1991,** *47*, 935.

153. Mathieu, H. J., Landolt, D., Schumacher, R., *Wear* **1986,** *110*, 61.

154. Shankwalkar, S. G., Cruz, C., *Ind. Eng. Chem. Res.* **1994,** *33*, 740.

155. Shankwalkar, S. G., Placek, D. G., *Ind. Eng. Chem. Res.* **1992,** *31*, 1810.

156. Shankwalkar, S. G., Placek, D.G., *J. Synth. Lubr.* **1994,** *11*, 121.

157. Hendrix, J. E., Drake, G. L., *J. Appl. Polym. Sci.* **1972,** *16*, 257.

158. Kettrup, A., Ohrbach, K. -H., Matuschek, G., Joachim, A., *Thermochim. Acta* **1990,** *166*, 41.

159. Huang, M.-R., Li, X. -G., *J. Appl. Polym. Sci.* **1998,** *68*, 293.

160. Flynn, J. H., Wall, L. A., *Polymer Lett.* **1966,** *4*, 323.

161. Ozawa, T., *B. Chem. Soc. Jpn.* **1965,** *38*, 1881.

162. Ozawa, T., *J. Therm. Anal.* **1970,** *2*, 301.